Desalination and Water Treatment
www.deswater.com
doi: 10.5004/dwt.2023.29504

292 (2023) 185–205
April

Less energy and aluminum electrode consumption for fluoride removal using electrocoagulation process: optimization by one-way ANOVA analysis and experimental design

Zakia Zmirli[a], Slimane El Harfaoui[b], Ali Mohssine[b], Anas Driouich[b], Hassan Chaair[b,*], Brahim Sallek[a]

[a]*Laboratory of Advanced Materials and Process Engineering, Faculty of Sciences, Ibn Tofail University, BP 242, Kenitra, Morocco, emails: zakia.zmirli@iut.ac.ma (Z. Zmirli), brahimsallek@gmail.com (B. Sallek)*
[b]*Laboratory of Process Engineering and Environment, Faculty of Sciences and Technics of Mohammedia, Hassan II University of Casablanca, BP 146 Mohammedia 28 806, Morocco, emails: hassan.chaair@univh2c.ma (H. Chaair), slimane.elharfaoui-etu@etu.univh2c.ma (S. El Harfaoui), ali.mouhssine-etu@etu.univh2c.ma (A. Mohssine), anas.driouich-etu@etu.univh2c.ma (A. Driouich)*

Received 24 November 2022; Accepted 26 March 2023

ABSTRACT

This study has two main objectives. First, an evaluation of the effects of five operating parameters namely current density (CD), electrolysis time (t_e), pH, conductivity (σ_i) and stirring speed (SS) on the fluoride removal by electrocoagulation (EC) was conducted through one-way analysis of variance (ANOVA) strategy. Two more performance indicators namely energy consumption and loss of electro-dissolved aluminum electrode were considered. Second, development of three regression models to model and to determine the optimal conditions for electrochemical fluoride reduction process. To this end, EC experiments were carried in batch mode using stirred reactor with Al–Al monopolar configuration. One-way ANOVA results confirm that CD, t_e, pH, σ_i and SS have significant effects on reactor performance to reduce fluoride. Multiple regression analysis method demonstrates the reliability of the three developed model to predict the outcomes with respective R^2 values of 0.9879, 0.9949 and 0.9813 for fluoride removal efficiency, energy consumption and loss of electrode, respectively. Thus, EC can effectively bring down the fluoride concentration below permissible limits (1.4 mg·L^{-1}) under the optimal conditions. The later are reached when the reactor is stirred at a speed of 102 rpm and the electrochemical cell is operating under a current density of 40.76 A·m^{-2} for an electrolysis time of 23.38 min and the solution pH is adjusted to 7.17 and a conductivity of 2,374 μS·cm^{-1}. These conditions generate a low energy consumption (54.58 Wh·m^{-3}) and electrode loss equal to 25.51 × 10^{-3}%.

Keywords: Electrocoagulation; Fluoride removal; One-way analysis of variance modelization; Response surface methodology

1. Introduction

Fluoride is one of the components found in a wide range of rocks and minerals. Its presence in groundwater may occur generally by natural geological processes, such as mineral dissolution (fluorite (CaF_2), villiaumite (NaF), fluorapatite ($Ca_5(PO_4)_3F$) and weathering of minerals due to water-rock interactions [1] and rarely by anthropogenic activity such as industries wastewater discharge including glass manufacturing industries, semiconductor industries [2], steel and aluminum industries and certain fertilizers and pesticides containing F^- [3].

* Corresponding author.

1944-3994/1944-3986 © 2023 Desalination Publications. All rights reserved.

Furthermore, the occurrence of fluoride is typical of arid or semi-arid areas and desert zones. In these areas, mineral dissolution is enhanced in aquifers because water spends longer time interacting with minerals due to high evapotranspiration and low recharge rates of aquifers [4–7]. On the other hand, alkaline environmental conditions contribute to the groundwater fluoride enrichment [8]. The concentration of F^- recorded in various aquifers around the world is in the range of 2–10 mg·L^{-1} [3]. Although trace amounts of fluoride in drinking water is necessary for the mineralization of bones and for strengthening tooth enamel ($0.5 < [F^-] \leq 1.5$ mg·L^{-1}) [9,10]. Its excess in water reservoirs above the permissible limit suggested by the World Health Organization (WHO) in drinking water ($[F^-] \leq 1.5$ mg·L^{-1}) [11] contaminate aquifers and surface water, thereby causing serious ecological environment issues and irreversible health effects for the population that consumes it over prolonged periods [3,12]. Long-term intake of drinking water containing this hazardous inorganic pollutant has been related to severe health diseases, such as dental fluorosis and calcification of the ligaments, retarded growth of children, skeletal defects, infertility in women and Alzheimer's syndrome [10,11,13–16]; decline cognitive abilities [17]. People in arid and semi-arid regions worldwide are more vulnerable to these severe health problems owing to drinking unsafe water containing fluoride [6,7,10]. On the other hand, considering the continuous growth of the population, water shortages are undoubtedly expected in several areas, which intensified by hydric sources limitation. Additionally, 1.8 billion people use contaminated water, according to the World Health Organization [11]. This explains the growing interest in the development or the enhancement of attractive simple wastewater treatment method to avoid water scarcity and unsafe drinking water like water reservoirs containing hazardous inorganic (such as fluoride) [10].

In this context, a large range of conventional processes were deployed to reduce fluoride concentration in groundwater/wastewater such as adsorption [18,19]; chemical precipitation using lime or magnesium salts [20,21], co-precipitation and adsorption with alum [22,23], ion-exchange [24,25], electrodialysis [26,27], coagulation–electroflotation [28], membrane separation [29]. However, a deep insight into all these techniques reveals various limitations and drawbacks depending on environmental and economic considerations. For example, high treatment time and pretreatment of adsorbent before use are the major flaws of adsorption process [9]. Similarly, the membrane process is a high-cost technology that produces concentrated discharge and requires skilled labor [9]. Likewise, coagulation process generates secondary pollution due to large volume of sludge and its disposal [30]. Such disadvantages have led the scientific community to explore alternative methods to reduce fluoride from groundwater/wastewater for drinking or recycling purposes. Recently, the environmental sector has expressed a growing interest in using electrocoagulation process (EC) as a unification of several water treatment processes, for example, coagulation, sedimentation, flotation and oxidation [31], to effectively remove a wide-spectrum of pollutant from water and wastewater. In the same trend, EC has emerged in numerous studies as an attractive alternative to the conventional method for defluoridation and many of them deemed successful [32–35]. Fluoride removal from contaminated groundwater/wastewater can be accomplished using different electrode materials such as iron, aluminum, steel and combination of Fe–Al. Compared to iron, aluminum electrodes (Al) used in EC cells are more advantageous because regardless of the current, iron corrodes spontaneously in water with uncontrolled generation of iron coagulants [12]. Moreover, unlike iron ions, released aluminum ions (Al^{3+}) during EC are polymerized to metal species and, consequently, the presence of free Al^{3+} is limited [12]. During the EC process, the sacrificial aluminum electrode used is dissolved by anode oxidation to yield Al^{3+} ions which further react with hydroxide group to form amorphous metal hydroxides $Al(OH)_3$. Thus, fluoride can be eliminated either by forming $Al(OH)_{(3-x)}F_x$ precipitate as outlined below by chemical substitution between hydroxide and fluoride ions [Eq. (1)] or/and chemical adsorption [Eq. (2)] [36]:

$$n\mathrm{Al}^{3+}_{(\mathrm{aq})} + (3n-m)\mathrm{OH}^-_{(\mathrm{aq})} + m\mathrm{F}^-_{(\mathrm{aq})} \rightarrow \mathrm{Al}_n\mathrm{F}_m(\mathrm{OH})_{(3n-m)(s)} \quad (1)$$

$$\mathrm{Al}_n(\mathrm{OH})_{3n(s)} + m\mathrm{F}^-_{(\mathrm{aq})} \leftrightarrow \mathrm{Al}_n\mathrm{F}_m(\mathrm{OH})_{(3n-m))(s)} + m\mathrm{OH}^-_{(\mathrm{aq})} \quad (2)$$

The fluoride removal mechanisms depend not only on electrode material and subsequently the predominant species formed but on several operating parameters including reactor design, applied current density, electrolysis time, pH, supporting electrolyte, inter-electrode distance, initial fluoride concentration, etc. The misunderstanding of the operating parameters contribution and their mutual interactions in the EC process may result in process failure. Thus, using one-way analysis of variance (ANOVA) method allows to gain information about the main input (process variables) effect on the outputs. Nevertheless, the lack of interaction effects information when using one-way ANOVA approach led to recognize that this approach is not adequate for optimization process as dealing by numerous studies [37,38]. Modeling process involved the regression analysis to determine the interrelationships between independent variables (operating parameters) and dependent variable (response variable) that are related causally [39]. Regression models is a predictive modelling technique used in almost all sciences, especially in health research to build a simplified mathematical explanation among variables with two purposes: prediction and effect estimation [39]. There are different types of regression models. Linear regression is one of the most basic types of regression. It consists of a predictor variable and a dependent variable related linearly to each other. In case the data involves more than one independent variable, then linear regression is called multiple linear regression models. Logistic regression model is appropriate for modeling a binary outcome. This means when the dependent variable can have only two values. Ridge regression is another type of regression model used when there is a high correlation between the independent variables. Polynomial regression models in which we regress a dependent variable on powers of the independent variables. Parameters of the polynomial model are estimated using a least square method [39]. On the other

hand, the best suitable pollutant removal strategy for process optimization should take into consideration both environmental and economic considerations. Consequently, the effectiveness of the EC process in reducing fluoride in water requires simultaneously lower energy consumption and no-excessive metal ion production which can compromise water quality and human health [10].

The novelty of this work is the coupling between two statistical methods ANOVA and response surface methodology (RSM) to optimize the removal of fluoride. Minimizing the use of the aluminum electrode and energy is a combination which has not been widely studied to date in the literature for optimizing fluoride removal with response surface methodology. The prevalence of applying one-way ANOVA approach allows to highlight the justified experimental domain of the studied factors in order to optimize the studied responses. In addition, investigation for the optimal conditions for fluoride removal by electrocoagulation with the simultaneous aim in terms of consuming lowest amount of aluminum electrode and energy can be an attractive to obtain fluoride-free water. Hence, the study is outlined as follows: firstly, the effect of five operating parameters by one-way ANOVA method is evaluated on the efficiency fluoride removal, which includes current density, electrolysis time, pH, conductivity and stirring speed. Secondly, based on the one-factor-at-a-time (OFAT) results, the levels of the process variables were selected at five distinct levels. Then, central composite design (CCD) was used to determine the influence of the interaction between independent process variables, to predict the three responses of the system (fluoride removal efficiency, energy consumed and mass loss of electrode by generating the mathematical models. Lastly, RSM optimization method was successfully applied to determine the optimal operating parameters for the reduction of fluoride concentration in water with the lowest energy consumption and electrode loss.

2. Materials and methods

2.1. Reactor setup and experimental procedure

The reactor used in this study (Fig. 1) is a cylindrical reactor made of transparent Plexiglas. The internal diameter and height are 9.4 cm, with a working volume of 0.45 L. The reactor operates in batch mode. The mixing inside the reactor was performed using a Ruston type propeller stirrer with 3 cm of diameter and placed 3 cm from the bottom of the reactor. A pair of plate aluminum with the purity of 99.94%–99.95% (Si 0.2%–0.8%, Fe 0.7%, Cu 3.5%–4.5%, Mn 0.4%–1%, Mg 0.4%–1%, Cr 0.1%, Zn 0.25%), provided from Serima Industries, Morocco with the following dimensions: (10 cm length, 2 cm width and 0.2 cm thickness) is used as electrodes and placed in a monopolar-parallel arrangement. Aluminum has been selected as electrodes material owing to its high affinity for fluoride ions [40]. The electrodes were dipped 3.7 cm into the reactor allowing an active electrode area equal to 7.4 cm^2 and the corresponding S/V ratio is equal to 1.64 $m^2 \cdot m^{-3}$. A Plexiglas cover is placed above the reactor fixing an inter-electrode distance (d_{int}) of 6 mm. The electrodes are connected to the Metrix AX-321 power supply. The reactor was operated in galvanostatic mode, implying that the current was kept constant while the potential of the cell varied. A multimeter of the brand PeakTech 2010 DMM was used optionally to monitor the current applied during the experiment and the voltage cell was recorded over time and calculated using trapezoidal method.

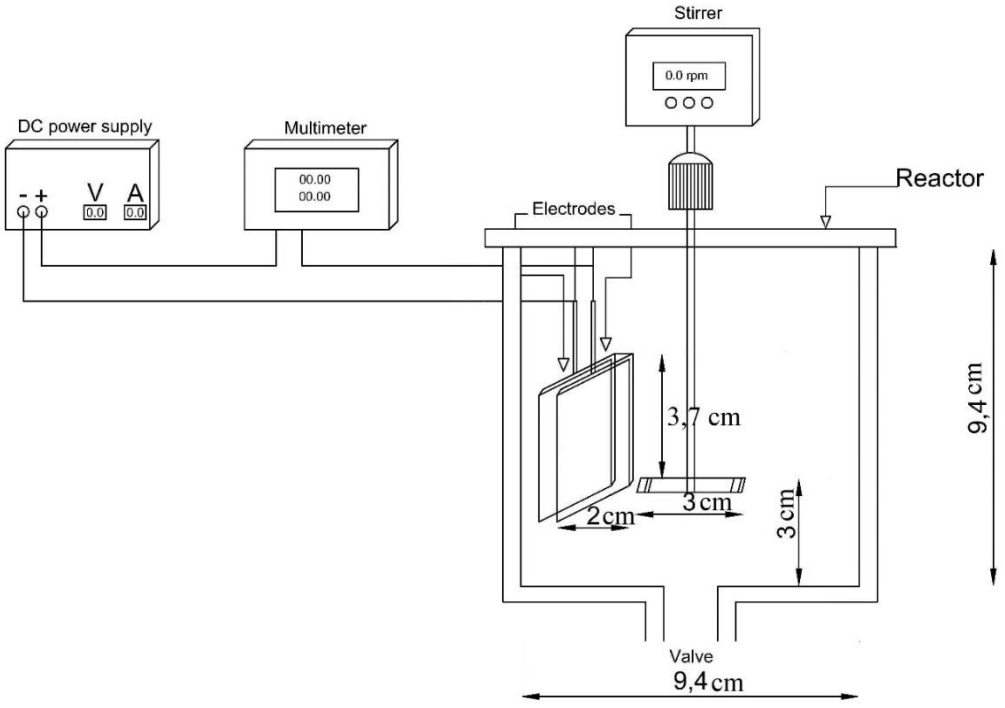

Fig. 1. Schematic representation of the electrochemical cell.

For each electrocoagulation experiment, the reactor is filled with a synthetic fluorine solution of fixed concentration, conductivity and pH. Electrolysis time and stirring speed of the mobile are set according to the conditions of each electrocoagulation experiment. At the end of the electrolysis time, a 50 mL volume of the treated solution is collected for analysis of the residual fluorine concentration. After every experiment, the electrodes are cleaned, dried and weighed to estimate the amount of dissolved aluminum of the electrodes.

2.2. Preparation of fluoride synthetic solution

Synthetic fluoride water was prepared by dissolving the desired amount of high purity NaF (from Sigma-Aldrich, USA) in distilled water to obtain a stock solution of 1 g·L^{-1}. Required concentration of fluoride to perform the EC tests was made from the dilution of stock solution in distilled water. All experiments were conducted with a fluoride synthetic wastewater of an initial concentration of $[F^-]_i$ = 7.27 mg·L^{-1}. According to each experimental test, potassium chloride was added to the fluoride solution to obtain the required conductivity (σ_i). Similarly, 0.1 N sodium hydroxide and 0.1 N hydrochloric acid solutions were added for pH adjustment.

2.3. Methods for measuring parameters

Conductivity-meter model HI-99300 HANNA (Italy) with a resolution of 1 μS·cm^{-1}, measure range of 0 to 3,999 μS·cm^{-1} and a pH-meter model Bante920 Benchtop (China) were used to measure conductivity and pH, respectively. Fluoride concentration is determined from through ionic activity (potential). This potential is measured by selective electrode connected to a potentiometer model HACK. The latter is translated into fluoride concentration based on the correlation according to calibration curve. The measure of the F^- ion activity requires the preparation of a TISAB solution (total ionic strength adjustment buffer) that is added to the samples to neutralize all interfering ions except F^-. TISAB solution was made from 500 mL of permuted water, 57 mL of acetic acid, 58 g of sodium chloride, 0.1 N NaOH to adjust the pH to 5 and 20 mL of citrate (prepared from 0.15 g sodium citrate dissolved in 100 mL of 1 N NaOH). TISAB solution was added to each sample with the volume ratio of 1:1, then stirred for at least 3 min before each potential measurement.

2.4. Performance analysis of the fluoride removal

The performance of the reactor has been evaluated based on the fluoride removal efficiency, the electrode loss and the energy consumption. Hence, Eq. (3) is used to calculate the fluoride removal efficiency in EC process as considered as the prime objective of water treatment for human consumption.

$$\text{Fluoride removal efficiency } (\%) = 100 \times \frac{\left[F^-\right]_i - \left[F^-\right]_f}{\left[F^-\right]_i} \quad (3)$$

where $[F^-]_i$ and $[F^-]_f$ represent the initial and final concentration of fluoride (mg·L^{-1}), respectively.

The energy consumption by electrocoagulation process for defluoridation of 1 m^3 of fluoride synthetic wastewater (Wh·m^{-3}) is expressed as follow:

$$\text{Energy consumption } \left(\text{Wh.m}^{-3}\right) = I \times \int_0^{t_e} \frac{U(t)dt}{V} \quad (4)$$

where I is the applied current (A), U represents the potential (V), t is the electrolysis time (h) and V refers to the volume of treated solution (m^3). The potential is recorded over electrolysis time and the energy consumption is calculated using trapezoidal rule method.

Since the pH of the samples used in this study is varied from acidic to neutral range, we cannot estimate the amount of dissolved electrode released from the anode by the general equation as indicated in Eq. (5). The latter is used only when the release of aluminium is purely electrochemical at the pH around 7. Hence, in our work, using the theoretical amount of aluminium is not suitable to determine the loss of electrode because of the simultaneous coexistence of the electrochemical and the chemical dissolution of aluminum due to the large range of pH studied. Hence, the amount of aluminium consumed was measured experimentally after each run. Aluminum electrode was cleaned using distilled water, dried at 105°C and kept at a desiccator for 15 min before weighing at OHAUS model balance to estimate the amount of dissolved of the electrodes. The electrode loss is then expressed as the difference mass of electrode before and after each electrocoagulation run [Eq. (6)].

$$m_{\text{th}}\left(\text{g/m}^3\right) = \frac{3{,}600 \times M_{\text{Al}} \times I}{z \times F \times V} \quad (5)$$

$$\text{Electrode loss}(\%) = 100 \times \left(\frac{m_i - m_f}{m_i}\right) \quad (6)$$

where m_{th} represent the theoretical amount of aluminum, M_{Al} is the molecular weight of aluminum (26.8 g·mol^{-1}), z is the number of electrons corresponding to aluminum oxidation (z = 3), F is the Faraday's constant (96,500 C·mol^{-1}), I is the applied current (A), V is the volume of treated solution (m^3), m_i and m_f are the aluminum weight measured before and after each run (g).

2.5. Data analysis

One-way analysis of variance (ANOVA) was conducted to investigate the effect of operational parameters to eliminate fluoride by EC. The parameters mainly taken into consideration are current density, pH, conductivity, electrolysis time and stirring speed. All measurements were expressed as calculated mean values for five replicates with standard errors (±S.E.). Then, the one-way analysis results have been used to conduct appropriate experiments to determine regression model equations and optimization conditions for fluoride removal by EC. In this step, three responses were considered: the fluoride removal efficiency, the energy consumption and the loss of electrode. Two steps are required for the process optimization. First, the estimation

of regression coefficients to develop an empirical model that correlates the responses to the factors that are proved to have a significant effect and predicts the responses at a point where no experiment has been performed [41,42]. Second, the application of the response surface methodology to carry out the optimum process parameters to remove the highest amount of fluoride with the lowest anode and energy consumption.

The Statistica [43] and JMP [44] statistical software's were used for regression analysis of experimental data to fit the equations developed and also to plot response surfaces. ANOVA was used to estimate the statistical parameters.

3. Results and discussions

The one-way ANOVA focuses on the evaluation of the effect of factors one by one on the fluoride elimination efficiency, setting at different level on the response while keeping all other factors at fixed values. Hence, electrocoagulation runs were performed in five replications to compute the mean value and standard deviation as follows:

- 5 levels for each factor except for the stirring speed (3 levels).
- 5 repetitions: every test during this study was repeated five times for all parameters to accurately measure and reduce the probable errors.

At the end of each EC run, the residual fluoride concentration was measured. The different levels of factors and the residual fluoride are summarized in Table 1. The reactor's performance at different level of factors is shown in Figs. 2 and 3.

3.1. Effect of current density, electrolysis time, pH, conductivity and stirring speed on reactor performance to remove fluoride

Figs. 2 and 3 display the average residual fluoride concentrations measured for the five variables current density (CD), t_e, pH, σ_i and stirring speed (SS).

One of the important parameters in EC process is the current density. The CD effect on EC performance in the reactor was investigated in the range of 20–60 A·m^{-2}. According to the result shown in Fig. 2a and Table 1, an overall decrease in fluoride concentration was observed with an increase in the current density set point. The highest reduction of 53% of fluoride was obtained at (CD = 60 A·m^{-2}) under the operational conditions indicated in Table 1. The same decreasing trend was found with increasing electrolysis time values until it reached a fluoride concentration of 2.58 mg·L^{-1} at t_e = 25 min (Fig. 2b).

Since it governs the species that are released during the electrocoagulation process and subsequently potential pollutant removal mechanisms, the pH parameter is crucially significant. The pH value also ranged from 4 to 8 (Fig. 2c) shows the changes in residual fluoride concentration with the input pH. However, fluoride removal efficiency had a strong inverse correlation to pH (Fig. 2c). The lowest residual fluoride concentration was achieved at pH 4 (2.15 mg·L^{-1}), which was significantly lower than at the other pH set point (5, 6, 7 and 8). With increasing the pH from 4 up to

Table 1
Range of factors and the average value of residual fluoride concentration

CD effect					
CD range (A·m^{-2})	20	30	40	50	60
Average value of $[F^-]_f$ (mg·L^{-1})	5.93	5.14	4.64	3.89	3.39
with $[F^-]_i$ = 7.27 mg·L^{-1}; t_e = 15 min; pH = 6; σ_i = 1,600 μS·cm^{-1}; SS = 150 rpm					
t_e effect					
t_e range (min)	5	10	15	20	25
Average value of $[F^-]_f$ (mg·L^{-1})	6.19	5.04	3.89	3.53	2.58
with $[F^-]_i$ = 7.27 mg·L^{-1}; CD = 50 A·m^{-2}; pH = 6; σ_i = 1,600 μS·cm^{-1}; SS = 150 rpm					
pH effect					
pH range	4	5	6	7	8
Average value of $[F^-]_f$ (mg·L^{-1})	2.15	2.78	3.46	3.65	6.01
with $[F^-]_i$ = 7.27 mg·L^{-1}; CD = 50 A·m^{-2}; t_e = 15 min; σ_i = 1,600 μS·cm^{-1}; SS = 150 rpm					
σ_i effect					
σ_i range (μS·cm^{-1})	800	1,600	2,400	3,200	4,000
Average value of $[F^-]_f$ (mg·L^{-1})	2.92	3.08	2.62	2.35	1.96
with $[F^-]_i$ = 7.27 mg·L^{-1}; CD = 50 A·m^{-2}; t_e = 15 min; pH = 7; SS = 150 rpm					
SS effect					
SS range (rpm)	50	150	250		
Average value of $[F^-]_f$ (mg·L^{-1})	2.51	3.08	2.61		
with $[F^-]_i$ = 7.27 mg·L^{-1}; CD = 50 A·m^{-2}; t_e = 15 min; pH = 7; σ_i = 1,600 μS·cm^{-1}					

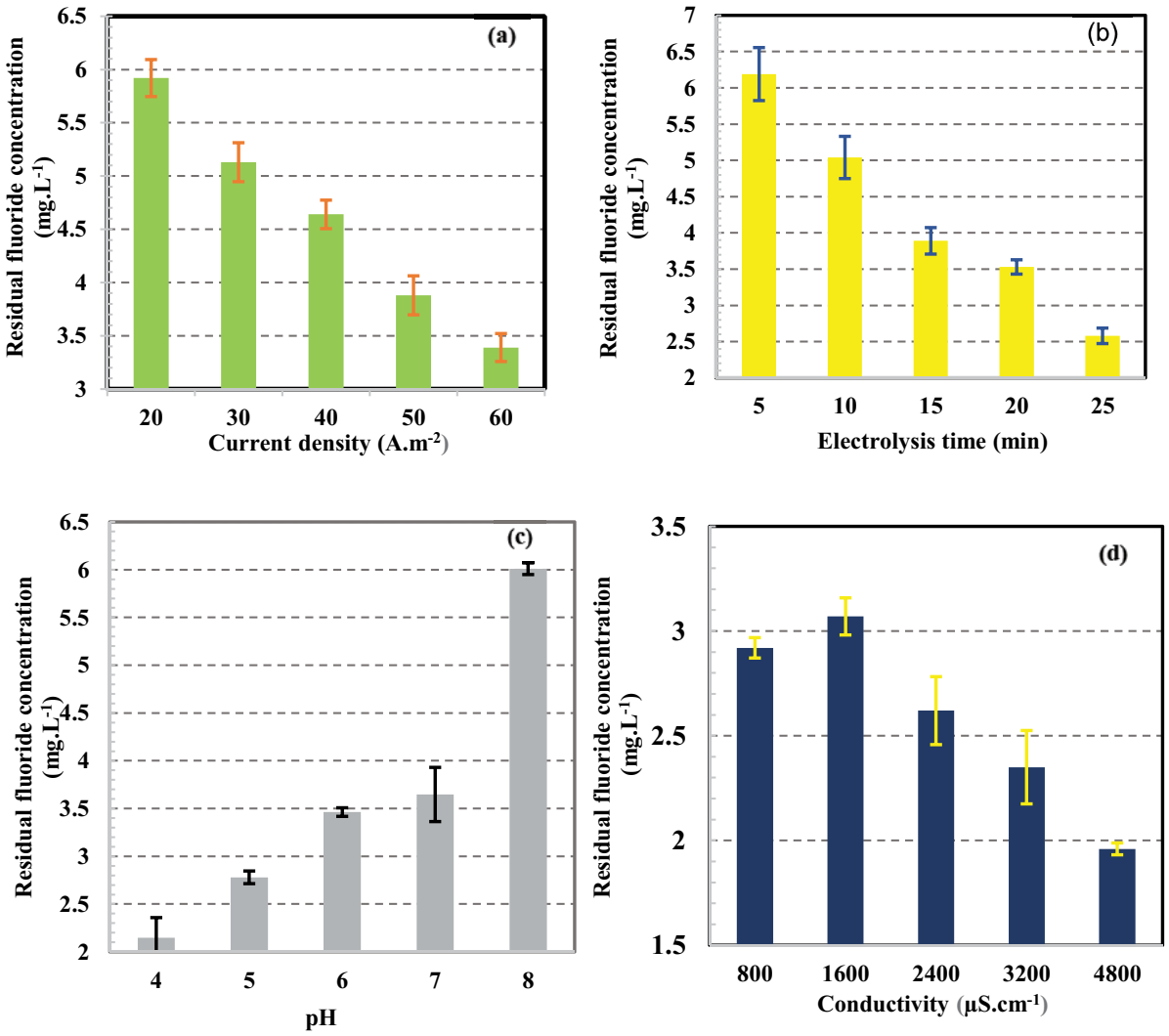

Fig. 2. Effect of CD, t_e, pH and σ_i on residual fluoride concentration. Data presented are mean values ±S.E. (n = 5).

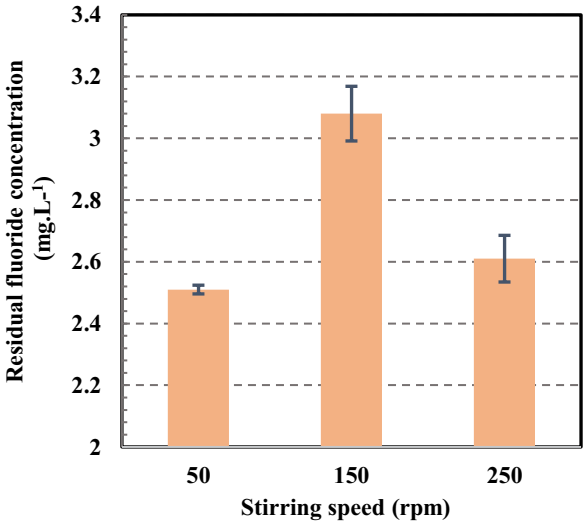

Fig. 3. Effect of SS on residual fluoride concentration. Data presented are mean values ±S.E. (n = 3).

8, fluoride removal efficiency was observed to gradually decrease from 70% to 17%.

The residual fluoride concentration was also measured for the five conductivity levels: 800; 1,600; 2,400; 3,200 and 4,000 µS·cm^{-1} (Fig. 2d). Except the small difference in residual fluoride concentration between the 800 and 1,600 µS·cm^{-1} conductivities (2.92 and 3.08 mg·L^{-1}), residual concentration of fluoride was found to decrease gradually over the others conductivity levels down to a minimum of 1.96 mg·L^{-1} of $[F^-]_f$ at σ_i = 4,000 µS·cm^{-1}.

The stirring speed effect on reactor performance was investigated in the range of 50, 150 and 250 rpm. Fig. 3 shows the average residual fluoride concentration measured for the three stirring speed levels. Based on these results, the fluoride removal was the highest (65.5%) when conducting (EC) experiments at 50 rpm of stirring speed.

3.1.1. Statistical analysis

The significance of the factors effects on the fluoride removal was further demonstrated through analysis of

variance (one-way ANOVA). The statistical analysis of electrocoagulation results by one-way ANOVA are listed in Table 2. If one-way ANOVA results in a p-value < 0.05, the null hypothesis is rejected, and it is revealed that there are significant differences between the elements [45]. Based on ANOVA results shown in Table 2, all p-values terms are less than 0.05. Hence CD, t_e, pH, σ_i and SS were found to have significant effects on reactor performance as significant differences were observed in residual fluoride concentration at the various range of CD, t_e, pH, σ_i and SS. In addition, F-test was applied to indicate whether a significant difference exists between the levels of a factor. Table 2 clearly shows that the F-value calculated experimentally (F_{exp}) for CD, t_e, pH an σ_i are equal to 189.7, 179.02, 399.29 and 73.83, respectively, which are higher than the value of critical Fisher–Snedecor factor for a confidence level of 95% ($F_{0.05}(4.20) = 2.87$) [46]. We can state that the F-value is sufficiently high to indicate statistical significance of factors on the fluoride removal. Similarly, Table 2 shows that the stirring speed is statistically significant factor as F-experimental value ($F_{exp} = 100.77$) is higher than the value of critical Fisher–Snedecor factor for a confidence level of 95% ($F_{0.05}(2.12) = 3.89$) [46].

3.1.2. Effect of current density

Current density (CD) is one of the parameters which strongly affect the electrocoagulation process efficiency. This parameter enhances the amount of electro-dissolved metallic cations and hydrogen gas bubble production and the flocs' growth in the reactor [14,31,47–49]. Hence, the increase of current density increased the sacrificial anode consumption and flocs formation which subsequently enhanced the pollutant removal [50]. Our findings align with the literature. The electrocoagulation tests conducted at current density of 20, 30, 40, 50 and 60 A·m^{-2} showed that defluoridation efficiency positively and proportionally correlate with the current density applied. It was observed that when the current density was increased by three times (from 20 to 60 A·m^{-2}), fluoride removal followed the same trend as it was increased from 18% to 53% The same observations were reported when conducting defluoridation process to remove 10 mg·L^{-1} of fluoride, at pH = 6 and 25 min of electrolysis time [14]. These authors indicated that increasing current density from 10 to 30 A·m^{-2} reduced the fluoride concentration from about 96% to 98.9% [14]. The fluoride removal efficiency was positively correlated with the applied current density [35]. This could be explained by the fact that the amount of in-situ coagulant $Al(OH)_3$ formed is affected by the applied cell potential which influences greatly the flocs' growth and the bubble size [35]. The evolution of fluoride concentration during EC in the stirred reactor was measured at different current and electrolysis times and the increase in applied current from 0.5 to 3 A favors the removal of fluoride in a shorter time [51]. However, they reported that defluoridation did not show a proportional increase with current when it is higher than 2 A and suggested that there is probably a transition between a domain of current in which the kinetics of Al electrolysis is the limiting step and another domain in which fluoride removal is limited either by the mechanisms of defluoridation or by other physical mechanisms, such as mixing [51].

3.1.3. Effect of electrolysis time

An incremental decrease in residual fluoride concentration was observed with an increase in electrolysis time. Fluoride removal is observed as 14%, 30%, 46%, 51% and 64% at t_e = 5, 10, 15, 20 and 25 min, respectively. The increase of electrolysis time from 5 to 25 min increased the fluoride removal by 4.5 times. It is ascribed to the continuous generation of the dissolved metal compounds from the anode

Table 2
Summary of analysis of variance for CD, pH, t_e, σ_i and SS

Factors	Source of variation	Sum of squares	Degree of freedom	Mean square	F_{exp}	p-value	Significance
Current density	Between groups	20.06936	4	5.01734	189.7006	1.34E-15	*
	Within groups	0.528975	20	0.026449			
	Total	20.59833	24				
Electrolysis time	Between groups	39.15093	4	9.787733	179.0165	2.35E-15	*
	Within groups	1.0935	20	0.054675			
	Total	40.24443	24				
pH	Between groups	43.04661	4	10.76165	399.2895	9.1E-19	*
	Within groups	0.53904	20	0.026952			
	Total	43.58565	24				
Conductivity	Between groups	4.018033	4	1.004508	73.82811	1.09E-11	*
	Within groups	0.272121	20	0.013606			
	Total	4.290153	24				
Stirring speed	Between groups	0.924928	2	0.462464	100.7694	3.15E-08	*
	Within groups	0.055072	12	0.004589			
	Total	0.98	14				

*significant to 95% ($F_{0.05}(4.20) = 2.87$);
*significant to 95% ($F_{0.05}(2.12) = 3.89$) [46].

per unit volume of solution and time inside the reactor and initial pH level. Long electrolysis time leads to higher contact time between contaminant and coagulant, which results in a high removal of fluoride [30,35]. Moreover, the required electrolysis time to remove fluoride from water depends on its initial concentration. The electrolysis time required to achieve a permissible residual fluoride concentration increased with the initial fluoride concentration [14,51]. At the operating conditions of the present runs, 25 min of treatment was not enough to reach the fluoride permissible concentration required by WHO guidelines (1.5 mg·L^{-1}) [11]. Consequently, the increase of electrolysis time to remove fluoride under 1.5 mg·L^{-1} is needed.

3.1.4. Effect of pH on fluoride removal efficiency

Considering the electrocoagulation process, it has been reported by several researchers that process performance for fluoride elimination is mainly dependent on initial pH [14,51]. The initial pH governs the rate of fluoride removal as it determines the predominant metal species formed and consequently the possible mechanism that occurs. In general, there would be a preferred operating pH to form the adequate metal species from the generated dissolved aluminum to promote destabilization and the removal of pollutant. On this basis, the effect of initial pH on the fluoride removal samples was investigated in the range of 4–8 and the residual fluoride concentration was found to be inversely correlated to the initial pH of the solution. The removal efficiency of fluoride was highest at the pH = 4 set point (70%), possibly due to the higher amount of hydroxy aluminum at this pH as compared to others. The initial pH of 4–5 allows the maximum fluoride removal efficiency as early reported [51] while other research works have shown that the maximal defluoridation by EC in a continuous mode is achieved with a neutral pH range of 6–8 [52]. The good performance obtained in a slightly acidic and neutral medium could be firstly attributed to the formation of positively charged monomeric and polymeric aluminum hydroxo complexes as well as the amorphous solid $Al(OH)_3$ (sweep-flocs). Then, the freshly formed flocs are polymerized to $Al_n(OH)_{3n}$ with a large surface area. Thus, fluoride is removed by chemisorption with a hydroxyl group [30].

The downward trend in fluoride elimination with an increase in pH samples aligned well with several research results [14,51,53]. The decrease of fluoride removal when pH ≥ 8 could be explained by the repulsive force between fluoride negatively charged and soluble negatively charged $Al(OH)^-_4$ and AlO^-_2 which causes a decrease of destabilization capacity for negatively charged colloids [10,54]. Therefore, to remove fluoride, sweep coagulation along with co-precipitation predominates [30,55].

3.1.5. Effect of solution conductivity

In the EC process, the electrolytic conductivity is one of the operating parameters that plays an important role in the process performance. Conductivity is a major factor that mainly affects the ohmic drop to transfer, the formation of oxide layer and consequently the efficiency, the energy consumption and the cost of the treatment. EC tests performed using synthetic water require the addition of a supporting electrolyte while groundwater/wastewater usually displays high electrolytic conductivity [10].

Based on the above results, except the low difference in fluoride concentration observed where increasing conductivity from 800 to 1,600 (2.92 and 3.08 mg·L^{-1}). It can be perceived that the increase of removal efficiency is noticed with the increase in samples conductivity and is found as 57%, 64%, 67.7% and 73% at different conductivity of 1,600; 2,400; 3,200 and 4,000 μS·cm^{-1}, respectively. It is attributed due to the presence of Cl^- ions in solution which ease the flow of electric current by stimulating the localized attack of the (hydr)oxide passivation layer from the working electrode surface, thus enhancing the chemical dissolution of aluminum anode into the solution and stable coagulating agents increases, which remove more contaminants and results in a high percentage removal of fluoride [56–58].

Regarding the positive effect of conductivity to prevent the formation of the anodic passivation layer during EC process, a gradual increase in the formation rate of stable coagulating agents by removing the oxyhydroxide species from the anode surface is observed [58–60]. This may be explained by the exchange reactions occurring between hydroxides and supporting electrolyte ions (Cl^-) and the additional formation of stable coagulating agents [60]. The addition of 0.71 g·L^{-1} NaCl to synthetic water with a fluoride initial concentration 12 mg·L^{-1} at pH = 7 was an effective way to achieve removal efficiencies of 87.5% [61]. Similarly, another study showed that the maximum fluoride removal efficiency was reached by adding a 0.05 M sodium chloride solution to the solution. Above this salt concentration, the fluoride removal efficiency decreased [62].

Based on the results above, an optimal value of salt concentration exists that may be suitable to meet the maximum inorganic toxin removal efficiency.

3.1.6. Effect of stirring speed

The design of the electrocoagulation reactor is considered one of the critical parameters in achieving optimal water treatment since it affects gas bubbling accumulation (oxygen and hydrogen), ohmic drop, stagnant zone, mass transfer inside the reactor and flotation/settling qualities [10]. In the present study, the cylindrical reactor with concentric parallel inner electrodes and rotating propeller (Fig. 1) is used. This geometry of EC reactor has been most widely used in EC [63–66]. The mixing mode is one of the several aspects that influence the entire functioning of electrochemical cell set-up [67]. The aim of this part is to assess how fluoride removal efficiency evolved when the stirring speed of rotating propeller change. Based on the results shown in Table 1, the stirring speed (SS) have a significant effect on the electrochemical reduction of fluoride. The highest fluoride reduction (65%) achieved at the lowest SS (50 rpm) is higher than those found at the other SS set point (150 and 250 rpm). EC carried out at lowest rotation speed of the propeller would have contributed favorably to mass transport. At low stirring speed, the high contact time between the upward flow of the generated hydrogen bubbles and the flocs formed by the EC promotes the collision and the agglomeration of solid particles. The hydrogen

bubbles gas attached to the formed flocs, reduce their density and finally enhance their flotation on the free surface of the reactor. Furthermore, the increase of the stirring speed induces an increase in the mixture velocity which prevents a sufficient contact time between the pollutant, the formed metallic species and the ascending hydrogen bubbles inside the reactor. The flotation is therefore less efficient. Thus, for the same mixing time, fluoride removal decreases. However, other authors have reported different results when they studied the effect of rotation speed on fluoride removal by EC in the stirred tank reactor [51]. Surprisingly, the fluoride removal rate appeared to increase with increasing rotation speed (from 50 to 400 rpm). External mass transfer and removal efficiency were not significantly different when the rotational speed was above 200 rpm [51].

In this part, the effect of five processing parameters CD, t_e, pH, σ_i and SS on electrochemical fluoride removal has been investigated based on the well-known experimental OFAT experimental strategy. However, the one-way ANOVA approach does not provide the complete interaction effects of all the variables influencing the EC process. It would be necessary to add another promising tool that considers all interactions of inputs (independent variables) on the output (dependent variable) for further modeling and optimization of the process. Hence, RSM is used to model and optimize the electrochemical fluoride removal process as it is recognized as a systematic approach to investigate the significance and potential contribution of operating factors, as well as their interactions on process performance, to develop and explain an empirical model that optimally represents the system. Moreover, the factor ranges are selected according to the results obtained on the removal of fluoride by OFAT. The input parameters ranges were taken as: current density (36.59–63.41 A·m^{-2}), electrolysis time (4.61–23.39 min), pH (4.66–7.34), conductivity (1,200 and 2,400 μS·cm^{-1}) and stirring speed (50 and 250 rpm). Two more performance indicators (energy consumption and loss of electrode) are added to determine the optimal conditions with respect to the three responses.

3.2. Development of regression model equations, statistical analysis and validation

3.2.1. Statistical analysis and mathematical model development

RSM in conjunction with CCD was selected to analyze the relationship between the responses and the independent process parameters for fluoride removal by EC. CCD and RSM are considered as the most common mathematical and statistical technique applied in industrial research for process development [68]. The levels of the process variables were selected based on the results obtained by OFAT below. Five levels were used for independent variables: current density, electrolysis time and pH while two levels were selected for conductivity and stirring speed (Table 3). Fluoride removal efficiency, energy consumed and electrode loss were the selected responses (dependent variable). 24 statistically designed experiments with 16 factorials, 6 axials and 2 centers points according to CCD were executed (Table 4).

The results obtained from CCD were evaluated using a multiple regression analysis method to evaluate the regression quality of the three models fitted using *p*-value as an indicator of the significance. The selected factors for elaborated models are significant, if *p*-value of each regression is lower than 0.05 (5%). Analogously, for a confidence level ≥95%, the terms in the quadratic model with *p*-value < 0.05 (5%) are considered significant else, they are insignificant [69]. Regarding the model summary statistics showed in Table 5, the *p*-values are equal to 0.0012, 0.0002 and 0.0047, respectively, for the fluoride removal efficiency, energy consumption and electrode loss, which are strictly lower than the level of significance α (α = 0.05) demonstrate the appropriateness of the quadratic model to depict the relationship between the independent input variables and the three responses. The *F*-values in the present work were 23.5993, 54.8850 and 13.3222 for the fluoride removal, energy consumed and loss of electrode, respectively, implies the statistical significance of the model with a 95% confidence level.

Further, the significance of each model term on the three response was assessed using the *F*-ratio calculated experimentally (F_{exp}) and *p*-value. The term with the smaller *p*-value (<0.05) and the higher *F*-ratio depicts the more significant model term [69]. On this basis, Table 6 summarizes the *F*-values and *p*-values for all linear, quadratic and interaction effects of the parameters.

3.2.2. Statistical evaluation of the effects of factors for fluoride removal efficiency, energy consumption and electrode loss

It's noted that all linear effects except linear effect pH and the product (interaction) terms CD × pH and σ_i × SS, the quadratic terms pH × pH have a significant positive effect on the fluoride removal by EC. The *p*-value for linear and interaction effects is lower than 0.05, whereas t_e effect presents a *p*-value < .0001. The rest of the model terms are not statistically significant (*p*-values ≥ 0.05) Based on the *F*-values, the linear term of the t_e was the major factor that affected the fluoride removal followed by CD with an *F*-values equal to 288.81 and 37.59, respectively.

On the other hand, the model terms namely, linear effects of CD, t_e, σ_i and CD × t_e, CD × pH, t_e × σ_i interactions effect significantly affect the energy consumption (*p*-values < 0.05). None of the quadratic effects have a significant effect since their *p*-values are higher than 0.05. Similarly, t_e and CD are

Table 3
Real and coded factors used in the central composite design

Real variable (x_i)	Coded factors X_1, X_2, X_3, X_4, X_5				
	−α	−1	0	+1	+α
x_1: Current density (CD), A·m^{-2}	36.59	40	50	60	63.41
x_2: Electrolysis time (t_e), min	4.61	7	14	21	23.39
x_3: pH	4.66	5	6	7	7.34
x_4: Conductivity (σ_i), μS·cm^{-1}	1,200			2,400	
x_5: Stirring speed (SS), rpm	50			250	

X_i (i = 1, 2, 3, 4, 5): coded variables, $X_i = (x_i - x_0)/\Delta x_i$, where x_i is the real value of an independent parameter, x_0 is the value of x_i at the center point and Δx_i is the step range.

Table 4
Experimental matrix

Order		Process variables									
		Current density ($A \cdot m^{-2}$)		Electrolysis time (min)		pH		Conductivity ($\mu S \cdot cm^{-1}$)		stirring Speed (rpm)	
Logical order	Randomized order	X_1	x_1	X_2	x_2	X_3	x_3	X_4	x_4	X_5	x_5
1	5	–	40	–	7	–	5	–	1,200	+	250
2	1	–	40	–	7	–	5	+	2,400	–	50
3	6	–	40	–	7	+	7	–	1,200	–	50
4	11	–	40	–	7	+	7	+	2,400	+	250
5	23	–	40	+	21	–	5	–	1,200	–	50
6	15	–	40	+	21	–	5	+	2,400	+	250
7	20	–	40	+	21	+	7	–	1,200	+	250
8	18	–	40	+	21	+	7	+	2,400	–	50
9	2	+	60	–	7	–	5	–	1,200	–	50
10	7	+	60	–	7	–	5	+	2,400	+	250
11	14	+	60	–	7	+	7	–	1,200	+	250
12	22	+	60	–	7	+	7	+	2,400	–	50
13	9	+	60	+	21	–	5	–	1,200	+	250
14	8	+	60	+	21	–	5	+	2,400		50
15	12	+	60	+	21	+	7	–	1,200	–	50
16	13	+	60	+	21	+	7	+	2,400	+	250
17	24	–α	36.59	0	14	0	6	–	1,200	–	50
18	21	+α	63.41	0	14	0	6	–	1,200	–	50
19	16	0	50	–α	4.61	0	6	–	1,200	+	250
20	4	0	50	+α	23.39	0	6	–	1,200	+	250
21	17	0	50	0	14	–α	4.66	+	2,400	–	50
22	3	0	50	0	14	+α	7.34	+	2,400	–	50
23	19	0	50	0	14	0	6	+	2,400	+	250
24	10	0	50	0	14	0	6	+	2,400	+	250

the most significant parameters as indicated by their corresponding *F*-values 480.39, 195.74, respectively. As expected, σ_i significantly affects the energy consumed. The increase of solution conductivity prevents the formation of oxide layer, dwindles the IR-drop (resistance) between electrodes and, consequently, increases the cell potential at the same current density that diminishes the energy consumption and the process cost [10,59].

Analogously, Table 6 displays *F*-value and *p*-value for all linear, quadratic and interaction effects of the parameters for electrode loss. The statistical results clearly showed that the significant model terms on the loss of electrode are the linear effects t_e and CD, interaction effect $t_e \times \sigma_i$ and quadratic effect pH × pH with a *p*-values of <0.0001, 0.0018, 0.0062 and 0.0413, respectively. The remaining terms had no significant effect on the response as demonstrated by the higher *p*-values (≥0.05) of their corresponding terms. Furthermore, in the current study, t_e and CD exhibit the most effect on the loss of electrode with *F*-value of 176.40 and 36.87, respectively.

Thus, the factors considered non-significant can be eliminated and the relationship between the independent input variables and the output responses was predicted by fitting experimental results to three empirical second-order polynomial models as presented in Table 7. Positive coefficient implies that the parameter originates a positive effect on the process responses, whereas negative sign indicates a reduction effect on the process.

3.2.3. Validation of model adequacy

The CCD factor levels of the five process variables as well as the experimental data and the predicted data resulted from the RSM model obtained by Statistica [43] and JMP [44] software's are given in Table 8.

The optimization of the experimental process parameters without assessing the model's adequate fitness findings could be misleading and unsatisfactory. The plot of predicted responses derived from the equations (Table 7) vs. experimental (actual) responses is generally used to ascertain the adequacy of the model in predicting the response variables [70]. The three plots between predicted and experimental values for fluoride removal, energy consumption and electrode loss responses are depicted in Fig. 4. There appeared an alignment of point clouds along the 45 median line for the three responses. The plots verify the model's overall predictability. The coefficient of determination as a measure of the model's degree of fit were: 0.99, 0.98 and 0.98 for the

Table 5
Analysis of variance results for the response surface quadratic models of fluoride removal efficiency, energy consumption and electrode loss as a function of CD, t_e, pH, σ_i and SS

Source	Degree of liberty	Sum of squares	Mean square	F_{exp}	p-value	Significance
		Fluoride removal efficiency				
Model	18	5,245.0078	291.389	23.5993	0.0012	***
Residual	5	61.7370	12.347			
Total	23	5,306.7448				
R-square	0.98837					
R-square adjusted	0.946485					
		Energy consumption				
Model	18	29,591.761	1,643.99	54.8850	0.0002	***
Residual	5	149.766	29.95			
Total	23	29,741.527				
R-square	0.99496					
R-square adjusted	0.976836					
		Electrode loss				
Model	18	1,954.6679	108.593	13.3222	0.0047	***
Residual	5	40.7563	8.151			
Total	23	1,995.4242				
R-square	0.98					
R-square adjusted	0.906046					

***significant to 99% ($F_{0.01}$ (18.5) = 4.59) [46].

Table 6
Analysis of variance for the responses

Source	Fluoride removal efficiency		Energy consumption		Electrode loss	
	F_{exp}	p-value	F_{exp}	p-value	F_{exp}	p-value
Constant	–	–	–	–	–	–
CD	37.5873	0.0017	195.7416	<0.0001	36.8696	0.0018
t_e	288.8097	<0.0001	480.3926	<0.0001	176.4018	<0.0001
pH	0.3080	0.6028	0.2825	0.6178	3.7920	0.1090
σ_i	8.3936	0.0339	68.6422	0.0004	0.5497	0.4918
SS	8.5336	0.0330	0.9947	0.3644	4.0622	0.0999
CD × CD	0.0000	0.9995	2.5641	0.1702	2.8035	0.1549
CD × t_e	0.0372	0.8546	51.1256	0.0008	0.0179	0.8988
t_e × t_e	1.9316	0.2233	0.1652	0.7012	1.0518	0.3521
CD × pH	9.9444	0.0253	7.9333	0.0373	1.1366	0.3351
t_e × pH	0.0751	0.7950	0.7695	0.4205	5.5838	0.0645
pH × pH	6.7141	0.0488	0.0238	0.8835	7.4489	0.0413
CD × σ_i	0.0012	0.9740	2.5673	0.1700	2.1704	0.2007
t_e × σ_i	4.5455	0.0862	20.7173	0.0061	20.5648	0.0062
pH × σ_i	0.1989	0.6742	2.1253	0.2047	5.2075	0.0714
CD × SS	0.0349	0.8592	4.5629	0.0857	0.9179	0.3820
t_e × SS	0.2109	0.6653	0.0539	0.8256	0.0722	0.7989
pH × SS	0.5418	0.4947	5.0295	0.0750	2.2750	0.1918
σ_i × SS	10.4526	0.0231	2.5591	0.1706	0.3257	0.5929

Significative at 1% ($F_{0.01}$(1.5 = 16.26);
Significative at 5% ($F_{0.05}$(1.5 = 6.61).

Table 7
Three empirical models for fluoride removal efficiency, energy consumption and electrode loss

Fluoride removal efficiency (%) = $55.5992 + 5.09X_1 + 14.138X_2 + 2.46X_4 - 2.48X_5 - 2.81X_1X_3 + 4.25X_3X_3 + 2.75X_4X_5$
Energy consumption ($Wh{\cdot}m^{-3}$) = $50.168937 + 17.85X_1 + 27.97X_2 - 10.83X_4 + 9.80X_1X_2 - 3.86X_1X_3 - 5.8X_2X_4$
Electrode loss × 10^3 (%) = $15.406387 + 3.85X_1 + 8.43X_2 + 3.428X_3X_3 + 2.87X_2X_4$

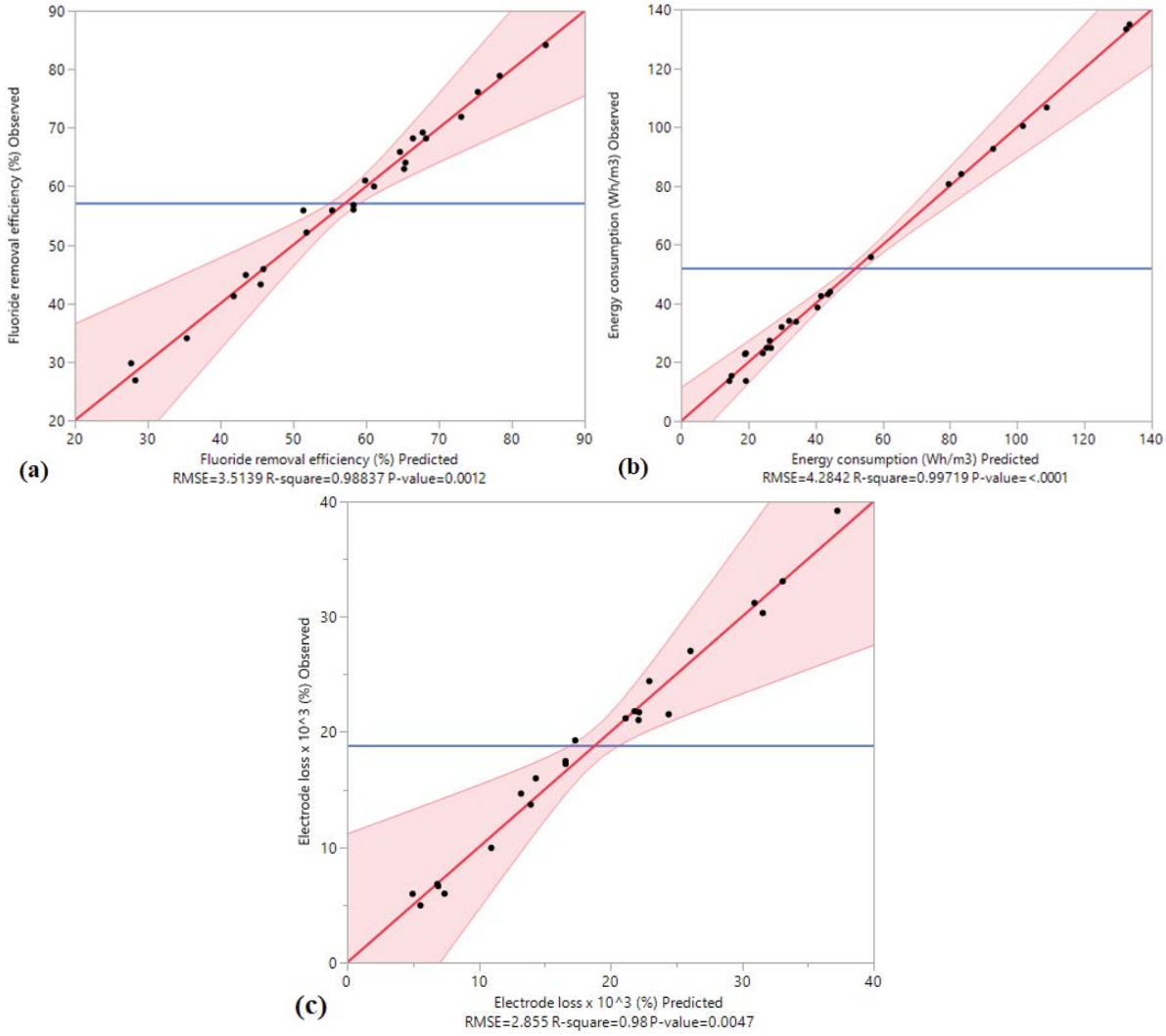

Fig. 4. Measured and predicted values of the developed models for (a) fluoride removal efficiency, (b) energy consumption and (c) electrode loss.

fluoride removal efficiency, energy consumption and electrode mass loss. These coefficients indicate how well a statistical model predicts an outcome. These coefficients will be closer to 1 the better a model well predict the responses. Therefore, the high value obtained of the coefficient of determination in this study corroborates that the quadratic models presented in Table 7 are able in predicting fluoride removal efficiency, energy consumption and electrode mass loss at studied experimental ranges. It has also been illustrated in Table 8 and Figs. 4 and 5 that the residuals values for the different responses selected are small and distributed randomly around zero which confirms the predictive accuracy of the three selected model with high precision.

3.3. Process optimization

The graphical representation of the established model in the space of variables allowed us to generate response surface graphs (three-dimensional graphs/3D) and iso-response curves (two-dimensional graphs/2D) The RSM 2 and 3-dimensional plots were built to determine the optimal values of operating EC process variables because it allows high

Table 8
Experimental and predicted responses values for fluoride removal efficiency, energy consumption and electrode loss

Standard order	Fluoride removal efficiency (%)		Energy consumption (Wh·m^{-3})		Electrode loss × 10^{-3}(%)	
	Experimental	Predicted	Experimental	Predicted	Experimental	Predicted
1	26.85	28.28	24.9	26.66	6.81	6.86
2	34.05	35.49	13.66	10.04	5.96	5.08
3	43.23	45.49	23.09	24.22	9.95	10.96
4	44.85	43.40	15.39	17.47	6.63	6.88
5	62.98	65.24	55.79	54.23	21.72	22.26
6	69.2	67.76	42.56	41.95	31.2	30.98
7	59.98	61.11	84.01	81.09	21.19	21.24
8	71.88	73.01	43.97	46.43	21.04	22.03
9	55.88	55.36	43.12	41.46	19.28	17.41
10	52.11	51.80	33.77	34.52	13.71	13.98
11	41.23	41.84	38.64	38.34	24.42	23.04
12	45.85	45.85	27.35	28.45	4.96	5.46
13	68.2	68.20	134.88	133.29	33.08	33.11
14	84.15	84.76	100.34	97.35	39.19	37.35
15	76.13	75.30	133.26	132.30	27.03	26.10
16	78.89	78.27	80.6	82.05	30.33	31.54
17	55.88	51.37	34.09	34.52	14.66	13.11
18	64.05	65.38	92.59	95.20	21.54	24.33
19	29.76	27.72	22.79	21.35	5.98	7.30
20	60.98	59.84	106.65	111.14	21.81	21.74
21	68.2	66.15	31.99	38.57	21.56	24.28
22	65.88	64.75	24.9	26.66	15.98	14.51
23	56.03	58.33	13.66	24.22	17.23	16.61
24	56.82	58.33	23.09	24.22	17.48	16.61

elucidation of interactive effects of independent parameters. Thus, the optimization was accomplished by RSM to identify the best combinations of the input parameters: CD, t_e, pH, σ_i and SS that led to the optimal electrochemical removal of fluoride, with the lower energy consumption and dissolved aluminum loss. Hence, the graphical optimization is presented in Figs. 6 and 7 which represent the interaction of the two independent variables (pH and CD) on the three responses when other variables are maintained at fixed levels (t_e = 23.38 min, σ_i = 2,374 μS·cm^{-1}, SS = 102 rpm). The interaction between current density vs. pH depicted in Figs. 6 and 7 clearly showed that CD have a positive great influence on the fluoride removal. At fixed value of pH, increasing CD favors continuous reduction of fluoride concentration with a minimal level of 68.71% and attain a maximum of 95.25%. It has been observed that increased CD was found to enhances the rate of dissolved metallic cations, regulates the size, up-growth and distribution of both flocs and gas microbubbles inside the reactor during EC and pollutant removal as a consequence through mass transport [50,70–72]. Other works reported that increasing current intensity depicts the supply of more energy to the EC reactor and would arise pollutant removal until reaching a constant value [70]. However, during the EC process, there is a limit current density above which two scenarios can occur: (i) flocs rupture by gas bubbling and (ii) excess of coagulation agents caused by the anode corrosion. Thus, the efficiency of pollutant removal can be negatively affected by these two scenarios [73]. Higher CD led to reduce the electrode lifetime [74]. Additionally, Figs. 6 and 7 depict the positive interaction of variables CD and pH in effecting the energy consumed during EC process from 30 to 116.44 Wh·m^{-3}.With the increase in the CD value at pH fixed value, while keeping the other variables constant at t_e = 23.38 min, σ_i = 2,374 μS·cm^{-1}, SS = 102 rpm, a gradual and considerable increase in the consumed energy was noted. An increase in the current density caused by a rise in the energy consumption has also been reported by some researchers [59,75–77]. This is explained by the use of higher cell potential at the same current density. On the other hand, according to the interaction between pH vs. CD on aluminum electrode loss response (Figs. 6 and 7), it was observed that the electrode weight loss increases by increasing CD at fixed pH set point, with a minimum loss corresponding to 26 × 10^{-3}%. This behavior might be attributed to the increase in the amount of dissolved metal ions from the sacrificial anode as applied current density increases [10,16,50,78]. Similar trend was observed by Moussavi et al. [48]. These authors experimentally measured both the loss weight of iron electrode and the cyanide removal efficiency for different current density. The results showed that the sacrificial anode (Fe) consumption was increased

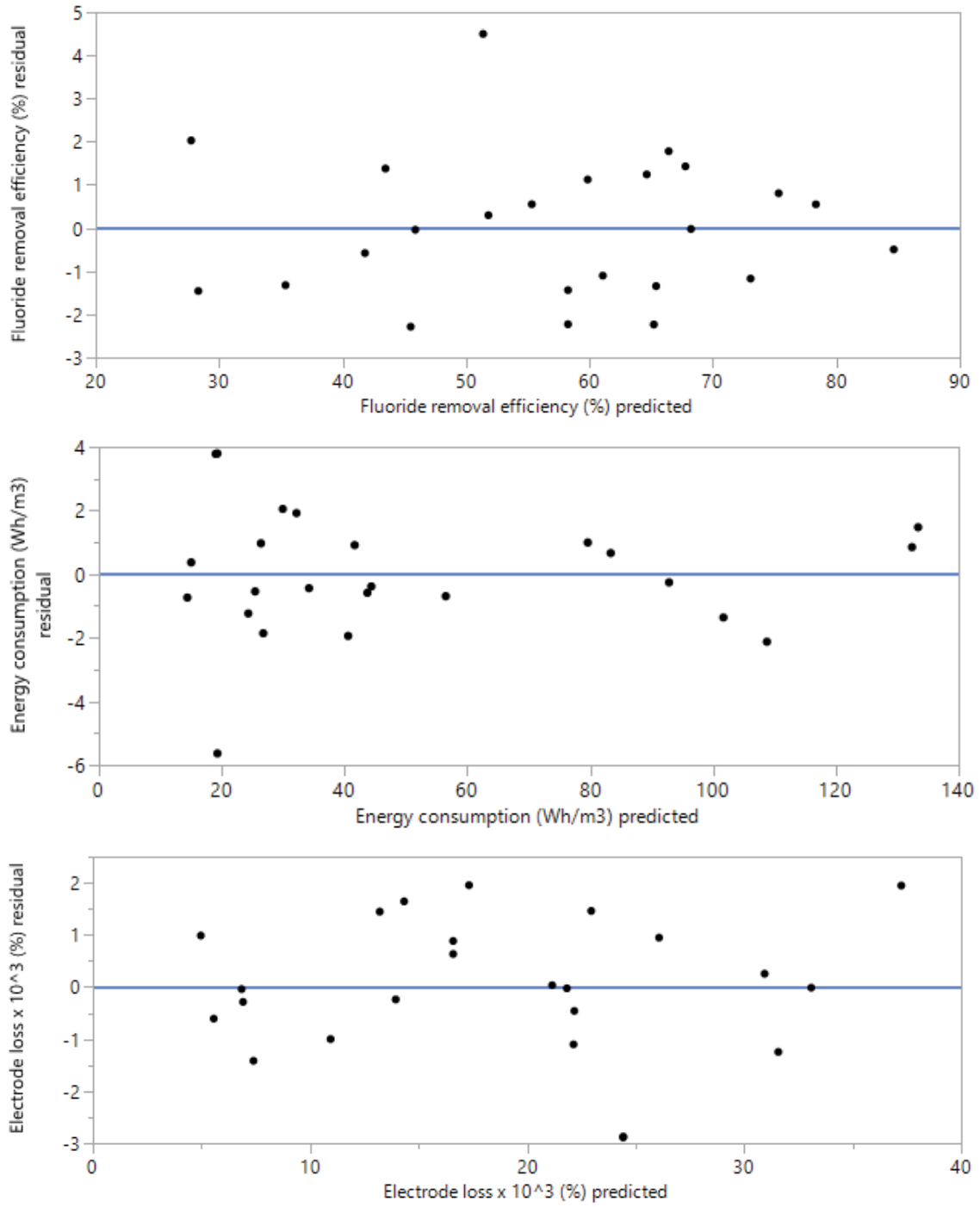

Fig. 5. Residual as function of predicted values for fluoride removal efficiency, energy consumption and electrode loss.

linearly by raising the current density from 2 to 150 A·m^{-2} leading to a complete cyanide removal [48].

Analogously, the effect of pH on the three responses is displayed in Figs. 6 and 7. Firstly, we have noted a different effect on fluoride removal when varying the pH level at fixed value of CD and keeping the other three variables constant (t_e = 23.38 min, σ_i = 2,374 µS·cm^{-1}, SS = 102 rpm). As shown in Figs. 6 and 7, increasing pH leads to a decrease in the percentage fluoride elimination until reaching a value and then continuous increasing of pH improves the fluoride removal efficiency. Considering the permissible limit of fluoride concentration suggested by the WHO, in drinking water (above 1.5 mg·L^{-1}) [11], we delimit the optimal domain of optimal fluoride removal that allows a removal efficiency of about 79%–80%. Furthermore, regarding the effect of pH on the energy consumption, it was observed that rising pH appeared to increase the consumed energy at CD fixed level. Hence, in order to identify the optimal domain of the

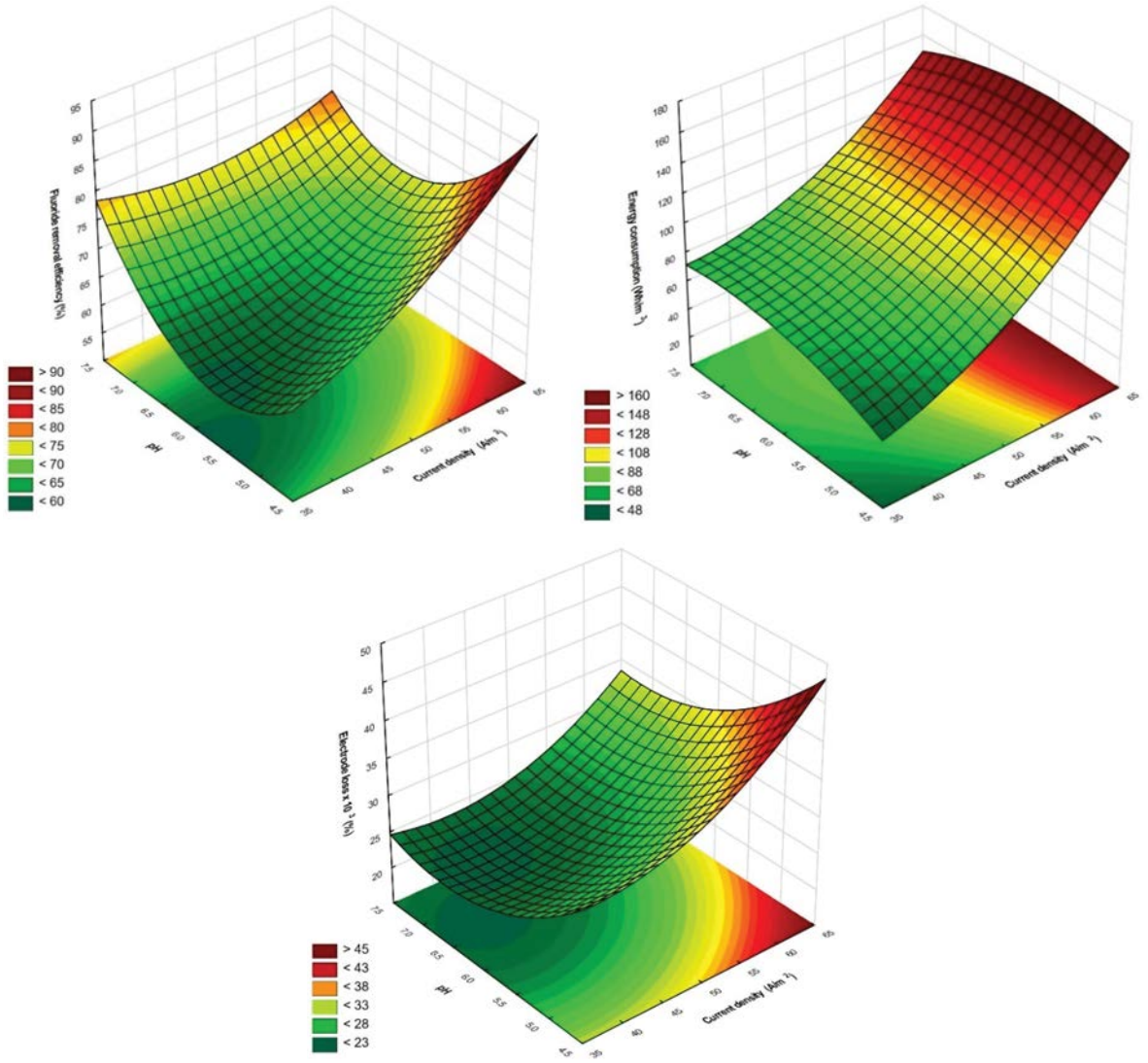

Fig. 6. Response surface of fluoride removal efficiency, energy consumption and electrode loss depending on CD and pH (t_e = 23.38 min; σ_i = 2,374 μS·cm^{-1}; SS = 102 rpm).

response, we need to minimize the energy consumed leading to desirable fluoride reduction (79%–80%). On the other hand, the two and three-dimensional plots depicted in Figs. 6 and 7 show the opposite effect of pH on electrode loss, at fixed CD set point, while the other variables were held constant. Figs. 6 and 7 show that at a fixed value of a CD, increase pH leads to decrease dissolved aluminum amount from 48.9 × 10^{-3} to 25.6 × 10^{-3}%. In addition, pollution reduction efficiency in EC process is directly related to the concentration of dissolved metal ions wish should be minimal to prevent a possible pollution production. This suggests minimizing the amount of aluminum (electrode loss) to remove about 79%–80% of fluoride by considering an optimal domain for both responses.

Similarly, the best combinations of the process variables for optimal fluoride by EC process requires acceptable fluoride removal efficiency based not only on environmental consideration but also on economic ones. Hence, a reduction in both energy consumption and amount of dissolved electrode are necessary. However, the response surface and iso-response plots showing the effects of CD and pH on fluoride removal, electrode loss and energy consumption in this study differ markedly. Because of these reasons, the best suitable pollutant removal strategy for process optimization implies appropriate investigation inside the iso-response plot of electrode loss corresponding to 26 × 10^{-3}% (minimal domain) to define the optimal domains of the variables to bring down the concentration of fluoride below permissible limits (1.5 mg·L^{-1}) with lower energy consumption.

The investigation results determined optimal domain of operating settings to bring down the concentration of fluoride as the WHO guidelines ([F$^-$] = 1.5 mg·L^{-1}) and simultaneously consuming moderate energy without excessive electrode loss. As depicted in the shaded portion (Fig. 7), the optimum region is covered by CD between 40.76

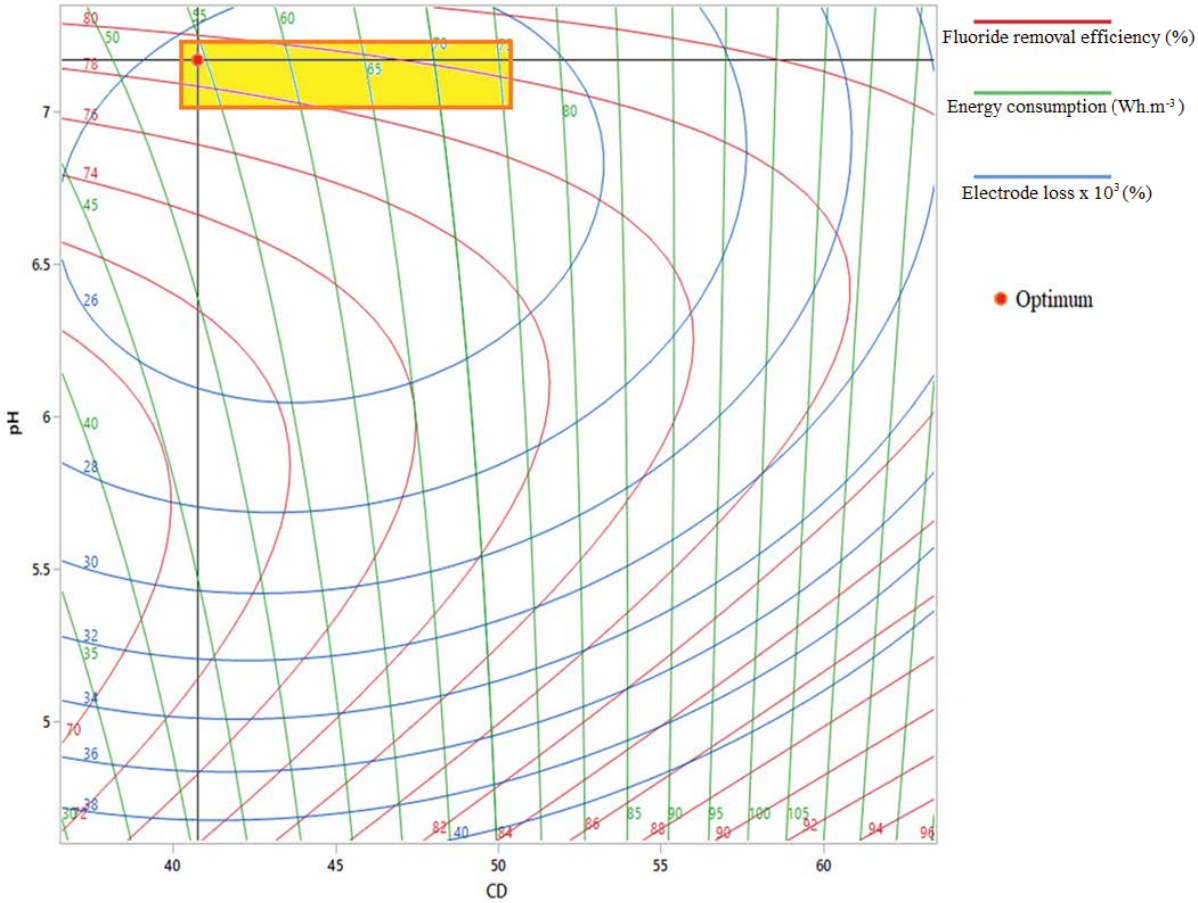

Fig. 7. Response surface and iso-response curves of fluoride removal efficiency, energy consumption and electrode loss depending on CD and pH (t_e = 23.38 min; σ_i = 2,374 μS·cm^{-1}; SS = 102 rpm).

and 50.24 A·m^{-2} and pH at the neutral range of 7.17–7.3 while keeping the other variables constant at 23.38 min, 2,374 μS·cm^{-1} and 102 rpm for t_e, σ_i and SS, respectively. The optimal conditions selected for the variables as well as the predicted value of three responses are outlined in Table 9.

Within the pH range of 7.17–7.3, permissible fluoride concentration is attained, which aligned well with the findings of other studies [30,79]. These researches confirmed that in a neutral pH and below pH = 8, the maximum removal efficiency is achieved, due to chemisorption of negatively charged fluoride on the positively charged species ($Al(OH)_2^+$) and neutral aluminum hydroxo species $Al(OH)_3$. This result coincides with some previously works that explored the influence of initial pH on defluoridation by EC process and reported that the optimal range of pH for maximum fluoride removal is 6–8 [52]. However, other researchers reported that fluoride removal is optimum in terms of retention time, energy requirements and aluminum mass consumption in acidic conditions (pH_i between 4 and 5) [51,56]. Table 9 shows that the current density (CD) and pH factors have a range of values in the optimal domain. As a result, to determine the optimal conditions for these values, we need to reduce the energy consumption as well as the electrode loss, therefore we should minimize the used current density. Table 10 summarizes the optimal conditions for each factor, as well as the predicted values of three responses. The optimum conditions for the RSM numerical optimization process were current intensity of 40.76 A·m^{-2}, pH of 7.17, electrolysis time of 23.38 min, 2,374 μS·cm^{-1} of conductivity and stirring speed of 102 rpm which culminated in optimal percentage fluoride removal of 79% consuming a total of 54.58 Wh·m^{-3} energy and 25.51 × 10^{-3}% as sacrificial aluminum electrode loss.

3.3.1. Experimental validation, characterization of the treated fluoride solution

The predicted data were compared by performing three experiments at the predicted optimum process parameters derived from RSM methodology CD = 40.76 A·m^{-2}, pH = 7.17, t_e = 23.38 min, σ_i = 2,374 μS·cm^{-1} and SS = 102 rpm. Overall, the validated experiment gave an average percentage fluoride removal value of 80.12% ($[F^-]_f$ = 1.4 mg·L^{-1}) an energy consumption of 50.72 Wh·m^{-3} and 26 × 10^{-3}% of electrode loss (Table 11). On comparing the experimental values with predicted responses, an error was found to be 1.12, –3.86 and 0.49 for fluoride removal, energy consumption and electrode loss, respectively; this means that the experimental and model results are in close agreement.

In addition, the characterization of the fluoride treated solution at the end of EC experiment at optimal conditions

Table 9
Optimal domain for maximal fluoride removal efficiency, minimum energy and electrode loss

Optimal domain of variable			Optimal responses		
	Min.	Max.		Min.	Max.
CD ($A \cdot m^{-2}$)	40.76	50.24	Fluoride removal efficiency (%)	79	81.89
pH	7.17	7.3	Energy consumption ($Wh \cdot m^{-3}$)	54.58	75.97
t_e (min)	23.38		Electrode loss × 10^{-3} (%)	25.51	26
σ_i ($\mu S \cdot cm^{-1}$)	2374				
SS (rpm)	102				

Table 10
Optimum values of the process parameters and predicted responses

Parameter	Optimum values	Predicted responses		
		Fluoride removal efficiency (%)	Energy consumption ($Wh \cdot m^{-3}$)	Electrode loss × 10^3 (%)
CD	40.76 $A \cdot m^{-2}$	79	54.58	25.51
pH	7.17			
t_e	23.38 min			
σ_i	2,374 $\mu S \cdot cm^{-1}$			

Table 11
Experiments validation at optimal operating conditions predicted by response surface methodology

Responses	Experimental value	Model response	Error
Fluoride removal (%)	80.12	79	1.12
Energy consumption ($Wh \cdot m^{-3}$)	50.72	54.58	–3.86
Electrode loss × 10^3 (%)	26	25.51	0.49

is presented in Table 12. A slight increase at final pH was observed (pH_f = 8.8) due to the generation of hydroxyl ions in the solution, that is, small amount of acid is needed to neutral pH at the end of the EC experiment.

Based on the experimental results of fluoride removal using EC in the previous study, the maximum fluoride removal efficiency was performed under the same optimum pH of the current result (pH = 7) [30,75,80,81]. The greater performance of fluoride removal ($[F^-]_f$ = 1.4 $mg \cdot L^{-1}$) can be explained by the mechanism involved during EC experiments under actual optimal pH (pH = 7.17) and the material used as sacrificial anode. Aluminum is suitable electrode material to remove fluoride from groundwater/wastewater as confirmed by the results obtained and reported by several works in the literature [12,35,61,79,82]. Aluminum has a high affinity for fluoride ions [40]. The investigation of various Al/Fe electrode configurations (4 Fe electrodes, 4 Al electrodes and 3/1 Al/Fe electrodes) to remove fluoride from synthetic water revealed that using only aluminum electrodes resulted in the highest fluoride removal efficiency (89%) [79]. However, this efficiency was decreased to 8.1% when using iron electrodes [79]. It has been well established that employing iron electrodes is not common for fluoride from water due to its low removal efficiency, which is sometimes not enough to meet the WHO recommendation (≤1.5 $mg \cdot L^{-1}$) [10]. Aluminum electrodes are the most efficient at removing fluoride, followed by aluminum alloys, an Al–Fe combination and Fe electrodes [3]. In the pH range of 7–8 aluminum exists predominantly as positive charged species $Al(OH)_2^+$ and $Al(OH)^{2+}$along with neutral species $Al(OH)_3$, that polymerized to dense floc $Al_n(OH)_{3n}$. The latter have low solubility and a large surface area that aid the fluoride removal [30,35,81]. Hence, negatively charged fluoride can be removed by chemisorption on the positively charged surface of the coagulants as explained in the introduction section. This results in fluorohydroxide aluminum complex formation [30]. These proposed mechanisms for fluoride removal by EC may be supported by the characterization of the produced sludge of other researchers. The Fourier-transform infrared spectroscopy (FTIR) of

Table 12
Characterization of the treated fluoride solution

Physico-chemical characteristics	Value	Disposal limits values
$[F^-]_f$, $mg \cdot L^{-1}$	1.4	1.5
pH	8.8	5.5–8.5
Conductivity, $\mu S \cdot cm^{-1}$	2,460	–
Temperature, °C	21	30

Table 13
Comparison of present study with other optimum operating parameters for fluoride removal by electrocoagulation

Influent	Process/operation mode	Optimum operating conditions	$[F^-]_i$ ($mg·L^{-1}$)	$[F^-]_f$ ($mg·L^{-1}$)	References
Synthetic water	EC Batch	Current density: 40.76 $A·m^{-2}$; time: 23.38 min; pH: 7.17; σ_i = 2,374 $\mu S·cm^{-1}$; rpm: 102	7.27	1.4	Present study
Synthetic water	EC Batch	Current density: 35.3 $A·m^{-2}$; time: 52.2 min; pH: 6.5; σ_i = 970 $\mu S·cm^{-1}$	10	0.3	[12]
Groundwater	EC Batch	Voltage: 30 V; time: 30 min; pH: 6; σ_i = 1,767 $\mu S·cm^{-1}$	29.5	2.45	[35]
Synthetic water	EC Batch	Current density: 99 $A·m^{-2}$; time: 50 min; σ_i = 550–680 $\mu S·cm^{-1}$; pH: 7.5	16	1.12	[81]
Groundwater	EC Continuous	Current density: 100 $A·m^{-2}$; time: 10 min; pH: 7.8; σ_i = 2,320 $\mu S·cm^{-1}$; half-period of polarity reversal: 1 min	7.35	1.4	[86]
Synthetic water	EC Continuous	Current density: 100 $A·m^{-2}$; time: 95 min; pH: 7; NaCl: 0.71 $g·L^{-1}$; 400 rpm; flow rate: 0.88 $L·h^{-1}$	12	1.5	[30]

produced dried sludge during the fluoride electrocoagulation treatment using Al electrodes exhibited peaks at 3,446; 1,020 and 609 cm^{-1} related to H–O–H, Al–O and Al–F–Al bond stretching, respectively which confirmed the presence of fluoride complexes [83]. Similarly, FTIR analyze of produced sludge exhibited at 1,020; 1,640 and 646 cm^{-1} peaks characteristics of Al–O bond stretching and O–H bending and Al–F stretching, respectively which indicate that fluoride is linked with aluminum hydroxide complexes [30].

Even though higher fluoride removal can be attained by several sets of experiments as suggested by the model or under operating conditions found at previous studies (Table 13), it was essentially important to choose one of them that reduced the fluoride concentration just to a level recommended by WHO (1.5 $mg·L^{-1}$). Thus, the operating parameters combination selected in present study was preferred as it successfully offered fluoride reduction below permissible limits (1.5 $mg·L^{-1}$) at the minimal energy consumption and also using low amount of aluminum. The present work successfully reduced fluoride to 1.4 $mg·L^{-1}$ with 26×10^{-3}% aluminum amount loss at optimized operation condition. The aluminum mass consumed per F removed (Al/F) was very low and calculated to be 0.3 $mg·mg^{-1}$ at optimal conditions. Moreover, reducing the aluminum amount used as much as possible prevents its presence in treated fluoride solution above recommended limits. However, further research is needed to determine aluminum species present in water after fluoride removal by EC. Furthermore, the energy consumed at the optimal operating conditions (54.58 $Wh·m^{-3}$) to reduce fluoride below the concentration limit is very low when compared to different research results. The energy consumption for reducing 91.6% of fluoride by EC in a reactor of a three-cell stack was 6.7 $Wh·m^{-3}$ while 1.98 $Wh·m^{-3}$ of energy was required to remove 97% of fluoride [12]. In another studies, 370 $Wh·m^{-3}$ energy was used to remove 90% of fluoride in the serpentine reactor with six-cell stack [84] and 340 $Wh·m^{-3}$ energy consumed was required to reduce 76% of fluoride [85]. The above overall reported results affirmed the ability of EC process using Al–Al electrodes to remove fluoride under an optimal combination of operational parameters. The optimization process was reliably and successfully suitable for not only an economical removal of fluoride but the desired aim in the minimizing of the aluminum amount consumption was attended. Therefore, the modeling and optimization data provided in this study are important and can be useful for the design and operation of continuous EC fluoride removal.

4. Conclusion

This current work investigated the fluoride removal in a laboratory-scale EC process operating in batch mode. A combined one-way ANOVA and RSM approach has been used for the optimization of fluoride removal taking into consideration simultaneous less energy and electrode consumption.

The electrocoagulation runs performed according to one-way ANOVA method described the effect of five operating parameters CD, t_e, pH, σ_i and SS on electrochemical fluoride removal. Furthermore, one-way ANOVA results indicate that all p-values terms are less than 0.05. Hence CD, t, pH, conductivity and SS were found to have significant effects on reactor performance as significant differences were observed in residual fluoride concentration at the various range of the five factors.

Based on the results of a one-way ANOVA, RSM and CCD were used to optimize the electrochemical process (EC) for fluoride removal in the ranges of process variables: current density ($36.59 \le CD \le 63.41$ $A·m^{-2}$, electrolysis time ($4.61 \le 1\ t_e \le 23.39$ min), pH ($4.66 \le pH \le 7.34$), conductivity (1,200 and 2,400 $\mu S·cm^{-1}$) and stirring speed (50 and 250 rpm). Moreover, two more performance indicators (energy and electrode consumption) are added to find out the optimal conditions with respect to the three responses.

The three plots between predicted and experimental values for three responses verify the model's overall predictability as the coefficient of determination were: 0.99, 0.98 and 0.98, respectively for the fluoride removal efficiency, energy consumption and electrode loss. The investigation inside the RSM 2 and 3-dimensional graphs allowed

us to defines the optimal domains of the variables to bring down the concentration of fluoride below permissible limits (1.5 $mg \cdot L^{-1}$). Thus, the electrochemical reactor must operate at a current intensity of 40.76 $A \cdot m^{-2}$, a pH of 7.17, an electrolysis time of 23.38 min, a conductivity of 2,374 $\mu S \cdot cm^{-1}$ and a stirring speed of 102 rpm to achieve a fluoride removal that meets the permissible limit (1.4 $mg \cdot L^{-1}$) with minimum energy consumption of 54.58 $Wh \cdot m^{-3}$ and 25.51 × 10^{-3}% as the optimum electrode loss.

Fluoride removal by electrocoagulation has been successfully assessed in a batch mode. Upcoming research will be conducted to study the transposition from batch to continuous mode using the knowledge gained from this work.

Conflict of interest statement

The authors declare that they have no known competing financial interests or personal relationships that could have appeared to influence the work reported in this paper.

References

[1] R. Gupta, A.K. Misra, Groundwater quality analysis of quaternary aquifers in Jhajjar District, Haryana, India: focus on groundwater fluoride and health implications, Alexandria Eng. J., 57 (2018) 375–381.

[2] C.Y. Hu, S.L. Lo, W.H. Kuan, Y.D. Lee, Removal of fluoride from semiconductor wastewater by electrocoagulation–flotation, Water Res., 39 (2005) 895–901.

[3] L.F. Castañeda, J.F. Rodríguez, J.L. Nava, Electrocoagulation as an affordable technology for decontamination of drinking water containing fluoride: a critical review, Chem. Eng. J., 413 (2021) 127529, doi: 10.1016/j.cej.2020.127529.

[4] M. Currell, I. Cartwright, M. Raveggi, D. Han, Controls on elevated fluoride and arsenic concentrations in groundwater from the Yuncheng Basin, China, Appl. Geochem., 26 (2011) 540–552.

[5] M.T. Alarcón-Herrera, J. Bundschuh, B. Nath, H.B. Nicolli, M. Gutierrez, V.M. Reyes-Gomez, D. Nunez, I.R. Martín-Dominguez, O. Srace, Co-occurrence of arsenic and fluoride in groundwater of semi-arid regions in Latin America: genesis, mobility and remediation, J. Hazard. Mater., 262 (2013) 960–969.

[6] M. Hossain, P.K. Patra, Hydrogeochemical characterisation and health hazards of fluoride enriched groundwater in diverse aquifer types, Environ. Pollut., 258 (2020) 113646, doi: 10.1016/j.envpol.2019.113646.

[7] V. Kimambo, P. Bhattacharya, F. Mtalo, J. Mtamba, A. Ahmad, Fluoride occurrence in groundwater systems at global scale and status of defluoridation – state of the art, Groundwater Sustainable Dev., 9 (2019) 100223, doi: 10.1016/j.gsd.2019.100223.

[8] T. Rafique, S. Naseem, T.H. Usmani, E. Bashir, F.A. Khan, M.I. Bhanger, Geochemical factors controlling the occurrence of high fluoride groundwater in the Nagar Parkar area, Sindh, Pakistan, J. Hazard. Mater., 171 (2009) 424–430.

[9] Meenakshi, R.C. Maheshwari, Fluoride in drinking water and its removal, J. Hazard. Mater., 137 (2006) 456–463.

[10] M.A. Sandoval, R. Fuentes, A. Thiam, R. Salazar, Arsenic and fluoride removal by electrocoagulation process: a general review, Sci. Total Environ., 753 (2021) 142108, doi: 10.1016/j.scitotenv.2020.142108.

[11] WHO, Guidelines for Drinking-Water Quality, 3rd ed., World Health Organization, Switzerland, 2006, pp. 375–376.

[12] J.U. Halpegama, K.Y. Heenkenda, Z.G. Wu, K.G.N. Nanayakkara, R.M.G. Rajapakse, A. Bandara, A.C. Herath, X. Chen, R. Weerasooriya, Concurrent removal of hardness and fluoride in water by monopolar electrocoagulation, J. Environ. Chem. Eng., 9 (2021) 106105, doi: 10.1016/j.jece.2021.106105.

[13] N. Mameri, A.R. Yeddou, H. Lounici, D. Belhocine, H. Grib, B. Bariou, Defluoridation of septentrional Sahara water of north Africa by electrocoagulation process using bipolar aluminium electrodes, Water Res., 32 (1998) 1604–1612.

[14] K.S. Hashim, A. Shaw, R. Al Khaddar, M. Ortoneda Pedrola, D. Phipps, Defluoridation of drinking water using a new flow column-electrocoagulation reactor (FCER) – experimental, statistical, and economic approach, J. Environ. Manage., 197 (2017) 80–88.

[15] M. Vithanage, P. Bhattacharya, Fluoride in the environment: sources, distribution and defluoridation, Environ. Chem. Lett., 13 (2015) 131–147.

[16] D. Ghosh, C.R. Medhi, M.K. Purkait, Treatment of fluoride containing drinking water by electrocoagulation using monopolar and bipolar electrode connections, Chemosphere, 73 (2008) 1393–1400.

[17] J. Yuan, Q. Li, R. Niu, J. Wang, Fluoride exposure decreased learning ability and the expressions of the insulin receptor in male mouse hippocampus and olfactory bulb, Chemosphere, 224 (2019) 71–76.

[18] P. Loganathan, S. Vigneswaran, J. Kandasamy, R. Naidu, Defluoridation of drinking water using adsorption processes, J. Hazard. Mater., 248–249 (2013) 1–19.

[19] Y. Wang, N. Chen, W. Wei, J. Cui, Z. Wei, Enhanced adsorption of fluoride from aqueous solution onto nanosized hydroxyapatite by low-molecular-weight organic acids, Desalination, 276 (2011) 161–168.

[20] H. Huang, J. Liu, P. Zhang, D. Zhang, F. Gao, Investigation on the simultaneous removal of fluoride, ammonia nitrogen and phosphate from semiconductor wastewater using chemical precipitation, Chem. Eng. J., 307 (2017) 696–706.

[21] L. Wang, Y. Zhang, N. Sun, W. Sun, Y. Hu, H. Tang, Precipitation methods using calcium-containing ores for fluoride removal in wastewater, Minerals, 9 (2019) 511, doi: 10.3390/min9090511.

[22] T. Akafu, A. Chimdi, K. Gomoro, Removal of fluoride from drinking water by sorption using diatomite modified with aluminum hydroxide, J. Anal. Methods Chem., 2019 (2019) 4831926, doi: 10.1155/2019/4831926.

[23] S.S. Tripathy, J.-L. Bersillon, K. Gopal, Removal of fluoride from drinking water by adsorption onto alum-impregnated activated alumina, Sep. Purif. Technol., 50 (2006) 310–317.

[24] S. Meenakshi, N. Viswanathan, Identification of selective ion-exchange resin for fluoride sorption, J. Colloid Interface Sci., 308 (2007) 438–450.

[25] M.S. Onyango, Y. Kojima, O. Aoyi, E.C. Bernardo, H. Matsuda, Adsorption equilibrium modeling and solution chemistry dependence of fluoride removal from water by trivalent-cation-exchanged zeolite F-9, J. Colloid Interface Sci., 279 (2004) 341–350.

[26] Z. Amor, B. Bariou, N. Mameri, M. Taky, S. Nicolas, A. Elmidaoui, Fluoride removal from brackish water by electrodialysis, Desalination, 133 (2001) 215–223.

[27] N. Arahman, S. Mulyati, M.R. Lubis, R. Takagi, H. Matsuyama, The removal of fluoride from water based on applied current and membrane types in electrodialysis, J. Fluorine Chem., 191 (2016) 97–102.

[28] S. Aoudj, A. Khelifa, N. Drouiche, M. Hecini, Removal of fluoride and turbidity from semiconductor industry wastewater by combined coagulation and electroflotation, Desal. Water Treat., 57 (2016) 18398–18405.

[29] P.I. Ndiaye, P. Moulin, L. Dominguez, J.C. Millet, F. Charbit, Removal of fluoride from electronic industrial effluent by RO membrane separation, Desalination, 173 (2005) 25–32, doi: 10.1016/j.desal.2004.07.042.

[30] L.S. Thakur, H. Goyal, P. Mondal, Simultaneous removal of arsenic and fluoride from synthetic solution through continuous electrocoagulation: operating cost and sludge utilization, J. Environ. Chem. Eng., 7 (2019) 102829, doi: 10.1016/j.jece.2018.102829.

[31] T. Kim, T.-K. Kim, K.-D. Zoh, Removal mechanism of heavy metal (Cu, Ni, Zn, and Cr) in the presence of cyanide during electrocoagulation using Fe and Al electrodes, J. Water Process Eng., 33 (2020) 101109, doi: 10.1016/j.jwpe.2019.101109.

[32] S. Aoudj, A. Khelifa, N. Drouiche, M. Hecini, H. Hamitouche, Electrocoagulation process applied to wastewater containing dyes from textile industry, Chem. Eng. Process. Process Intensif., 49 (2010) 1176–1182.
[33] K.-J. Kim, K. Baek, S. Ji, Y. Cheong, G. Yim, A. Jang, Study on electrocoagulation parameters (current density, pH, and electrode distance) for removal of fluoride from groundwater, Environ. Earth Sci., 75 (2015) 45, doi: 10.1007/s12665-015-4832-6.
[34] S. Vasudevan, J. Jayaraj, J. Lakshmi, G. Sozhan, Removal of iron from drinking water by electrocoagulation: adsorption and kinetics studies, Korean J. Chem. Eng., 26 (2009) 1058–1064.
[35] R. Mureth, R. Machunda, K.N. Njau, D. Dodoo-Arhin, Assessment of fluoride removal in a batch electrocoagulation process: a case study in the Mount Meru Enclave, Sci. Afr., 12 (2021) e00737, doi: 10.1016/j.sciaf.2021.e00737.
[36] C.Y. Hu, S.L. Lo, W.H. Kuan, Y.D. Lee, Removal of fluoride from semiconductor wastewater by electrocoagulation–flotation, Water Res., 39 (2005) 895–901.
[37] V.A. Sakkas, Md. A. Islam, C. Stalikas, T.A. Albanis, Photocatalytic degradation using design of experiments: a review and example of the Congo red degradation, J. Hazard. Mater., 175 (2010) 33–44.
[38] T. Ntambwe Kambuyi, F. Eddaqaq, A. Driouich, B. Bejjany, B. Lekhlif, H. Mellouk, K. Digua, A. Dani, Using response surface methodology (RSM) for optimizing turbidity removal by electrocoagulation/electro-flotation in an internal loop airlift reactor, Water Supply, 19 (2019) 2476–2484.
[39] E. Ostertagová, Modelling using polynomial regression, Procedia Eng., 48 (2012) 500–506.
[40] S. Aoudj, A. Khelifa, N. Drouiche, M. Hecini, HF wastewater remediation by electrocoagulation process, Desal. Water Treat., 51 (2013) 1596–1602.
[41] H. Khoshvaght, M. Delnavaz, M. Leili, Optimization of acetaminophen removal from high load synthetic pharmaceutical wastewater by experimental and ANOVA analysis, J. Water Process Eng., 42 (2021) 102107, doi: 10.1016/j.jwpe.2021.102107.
[42] S. El Harfaoui, A. Driouich, A. Mohssine, S. Belouafa, Z. Zmirli, H. Mountacer, K. Digua, H. Chaair, Modelization and optimization of the treatment of the reactive black-5 dye from industry effluents using experimental design methodology, Sci. Afr., 16 (2022) e01229, doi: 10.1016/j.sciaf.2022.e01229.
[43] Statistica, C. WeißStatSoft, Inc., Tulsa, OK: STATISTICA, Version 8, AStA Adv. Statis. Anal. 91, 2007, pp. 339–341.
[44] JMP, SAS Institute Inc., JMP 10 Basic Analysis and Graphing, 2nd ed., USA, 2012.
[45] K.K. Boyer, J.R. Olson, R.J. Calantone, E.C. Jackson, Print versus electronic surveys: a comparison of two data collection methodologies, J. Oper. Manage., 20 (2002) 357–373.
[46] K.H. Esbensen, D. Guyot, F. Westad, L.P. Houmoller, Multivariate Data Analysis: In Practice: An Introduction to Multivariate Data Analysis and Experimental Design, Aalborg University, Esbjerg, Denmark, 2002.
[47] A. Shahedi, A.K. Darban, F. Taghipour, A. Jamshidi-Zanjani, A review on industrial wastewater treatment via electrocoagulation processes, Curr. Opin. Electrochem., 22 (2020) 154–169.
[48] G. Moussavi, F. Majidi, M. Farzadkia, The influence of operational parameters on elimination of cyanide from wastewater using the electrocoagulation process, Desalination, 280 (2011) 127–133.
[49] W. Balla, A.H. Essadki, B. Gourich, A. Dassaa, H. Chenik, M. Azzi, Electrocoagulation/electroflotation of reactive, disperse and mixture dyes in an external-loop airlift reactor, J. Hazard. Mater., 184 (2010) 710–716.
[50] U. Tezcan Un, A. Savas Koparal, U. Bakir Ogutveren, Fluoride removal from water and wastewater with a bach cylindrical electrode using electrocoagulation, Chem. Eng. J., 223 (2013) 110–115.
[51] A.H. Essadki, B. Gourich, Ch. Vial, H. Delmas, M. Bennajah, Defluoridation of drinking water by electrocoagulation/electroflotation in a stirred tank reactor with a comparative performance to an external-loop airlift reactor, J. Hazard. Mater., 168 (2009) 1325–1333.
[52] M.M. Emamjomeh, M. Sivakumar, Fluoride removal by a continuous flow electrocoagulation reactor, J. Environ. Manage., 90 (2009) 1204–1212.
[53] F. Shen, X. Chen, P. Gao, G. Chen, Electrochemical removal of fluoride ions from industrial wastewater, Chem. Eng. Sci., 58 (2003) 987–993.
[54] M.M. Emamjomeh, M. Sivakumar, A.S. Varyani, Analysis and the understanding of fluoride removal mechanisms by an electrocoagulation/flotation (ECF) process, Desalination, 275 (2011) 102–106.
[55] C.Y. Hu, S.L. Lo, W.H. Kuan, Effects of co-existing anions on fluoride removal in electrocoagulation (EC) process using aluminum electrodes, Water Res., 37 (2003) 4513–4523.
[56] M. Bennajah, B. Gourich, A.H. Essadki, Ch. Vial, H. Delmas, Defluoridation of Morocco drinking water by electrocoagulation/electroflotation in an electrochemical external-loop airlift reactor, Chem. Eng. J., 148 (2009) 122–131.
[57] G. Mouedhen, M. Feki, M.D.P. Wery, H.F. Ayedi, Behavior of aluminum electrodes in electrocoagulation process, J. Hazard. Mater., 150 (2008) 124–135.
[58] K. Mansouri, K. Ibrik, N. Bensalah, A. Abdel-Wahab, Anodic dissolution of pure aluminum during electrocoagulation process: influence of supporting electrolyte, initial pH, and current density, Ind. Eng. Chem. Res., 50 (2011) 13362–13372.
[59] S. Abbasi, M. Mirghorayshi, S. Zinadini, A.A. Zinatizadeh, A novel single continuous electrocoagulation process for treatment of licorice processing wastewater: optimization of operating factors using RSM, Process Saf. Environ. Prot., 134 (2020) 323–332.
[60] N. Drouiche, S. Aoudj, M. Hecini, N. Ghaffour, H. Lounici, N. Mameri, Study on the treatment of photovoltaic wastewater using electrocoagulation: fluoride removal with aluminium electrodes—characteristics of products, J. Hazard. Mater., 169 (2009) 65–69.
[61] L.S. Thakur, P. Mondal, Simultaneous arsenic and fluoride removal from synthetic and real groundwater by electrocoagulation process: parametric and cost evaluation, J. Environ. Manage., 190 (2017) 102–112.
[62] S. Aoudj, A. Khelifa, N. Drouiche, Removal of fluoride, SDS, ammonia and turbidity from semiconductor wastewater by combined electrocoagulation–electroflotation, Chemosphere, 180 (2017) 379–387.
[63] E. Demirbas, M. Kobya, M.S. Oncel, E. Şık, A.Y. Goren, Arsenite removal from groundwater in a batch electrocoagulation process: optimization through response surface methodology, Sep. Sci. Technol., 54 (2019) 775–785.
[64] M. Kobya, F. Ozyonar, E. Demirbas, E. Sik, M.S. Oncel, Arsenic removal from groundwater of Sivas-Şarkişla Plain, Turkey by electrocoagulation process: comparing with iron plate and ball electrodes, J. Environ. Chem. Eng., 3 (2015) 1096–1106.
[65] D. Lakshmanan, D.A. Clifford, G. Samanta, Comparative study of arsenic removal by iron using electrocoagulation and chemical coagulation, Water Res., 44 (2010) 5641–5652.
[66] S, Sen, A.K. Prajapati, A. Bannatwala, D. Pal, Electrocoagulation treatment of industrial wastewater including textile dyeing effluent – a review, Desal. Water Treat., 161 (2019) 21–34.
[67] P. Song, Z. Yang, G. Zeng, X. Yang, H. Xu, L. Wang, R. Xu, W. Xiong, K. Ahmad, Electrocoagulation treatment of arsenic in wastewaters: a comprehensive review, Chem. Eng. J., 317 (2017) 707–725.
[68] E. Nariyan, M. Sillanpää, C. Wolkersdorfer, Uranium removal from Pyhäsalmi/Finland mine water by batch electrocoagulation and optimization with the response surface methodology, Sep. Purif. Technol., 193 (2018) 386–397.
[69] C.E. Onu, J.T. Nwabanne, P.E. Ohale, C.O. Asadu, Comparative analysis of RSM, ANN and ANFIS and the mechanistic modeling in Eriochrome black-T dye adsorption using modified clay, S. Afr. J. Chem. Eng., 36 (2021) 24–42.
[70] C.C. Obi, J.T. Nwabanne, C.A. Igwegbe, P.E. Ohale, C.O.R. Okpala, Multi-characteristic optimization and modeling analysis of electrocoagulation treatment of abattoir

wastewater using iron electrode pairs, J. Water Process Eng., 49 (2022) 103136, doi: 10.1016/j.jwpe.2022.103136.
[71] U. Tezcan Un, A.S. Koparal, U. Bakir Ogutveren, Electrocoagulation of vegetable oil refinery wastewater using aluminum electrodes, J. Environ. Manage., 90 (2009) 428–433.
[72] M. Kobya, U. Gebologlu, F. Ulu, S. Oncel, E. Demirbas, Removal of arsenic from drinking water by the electrocoagulation using Fe and Al electrodes, Electrochim. Acta, 56 (2011) 5060–5070.
[73] M.A. Sandoval, R. Fuentes, J.L. Nava, I. Rodríguez, Fluoride removal from drinking water by electrocoagulation in a continuous filter press reactor coupled to a flocculator and clarifier, Sep. Purif. Technol., 134 (2014) 163–170.
[74] A.R. Anuf, K. Ramaraj, V.S. Sivasankarapillai, R. Dhanusuraman, J. Prakash Maran, G. Rajeshkumar, A. Rahdar, A.M. Díez-Pascual, Optimization of electrocoagulation process for treatment of rice mill effluent using response surface methodology, J. Water Process Eng., 49 (2022) 103074, doi: 10.1016/j.jwpe.2022.103074.
[75] M. Behbahani, M.R.A. Moghaddam, M. Arami, Techno-economical evaluation of fluoride removal by electrocoagulation process: optimization through response surface methodology, Desalination, 271 (2011) 209–218.
[76] P.I. Omwene, M. Kobya, Treatment of domestic wastewater phosphate by electrocoagulation using Fe and Al electrodes: a comparative study, Process Saf. Environ. Prot.,116 (2018) 34–51.
[77] M.A. Mamelkina, M. Herraiz-Carboné, S. Cotillas, E. Lacasa, C. Sáez, R. Tuunila, M. Sillanpää, A. Häkkinen, M.A. Rodrigo, Treatment of mining wastewater polluted with cyanide by coagulation processes: a mechanistic study, Sep. Purif. Technol., 237(2020) 116345, doi: 10.1016/j.seppur.2019.116345.
[78] M. Al-Shannag, Z. Al-Qodah, K. Bani-Melhem, M.R. Qtaishat, M. Alkasrawi, Heavy metal ions removal from metal plating wastewater using electrocoagulation: kinetic study and process performance, Chem. Eng. J., 260 (2015) 749–756.
[79] X. Zhao, B. Zhang, H. Liu, J. Qu, Simultaneous removal of arsenite and fluoride via an integrated electro-oxidation and electrocoagulation process, Chemosphere, 83 (2011) 726–729.
[80] Q. Zuo, X. Chen, W. Li, G. Chen, Combined electrocoagulation and electroflotation for removal of fluoride from drinking water, J. Hazard. Mater., 159 (2008) 452–457.
[81] M.J. Nyangi, Y. Chebude, K.F. Kilulya, M. Andrew, Simultaneous removal of fluoride and arsenic from water by hybrid Al-Fe electrocoagulation: process optimization through surface response method, Sep. Sci. Technol., 56 (2021) 2648–2658.
[82] M. Alimohammadi, A. Mesdaghinia, M.H. Shayesteh, H.J. Mansoorian, N. Khanjani, The efficiency of the electrocoagulation process in reducing fluoride: application of inductive alternating current and polarity inverter, Int. J. Environ. Sci. Technol., 16 (2019) 8239–8254.
[83] M. Changmai, M. Pasawan, M.K. Purkait, A hybrid method for the removal of fluoride from drinking water: parametric study and cost estimation, Sep. Purif. Technol., 206 (2018) 140–148.
[84] M.A. Sandoval, R. Fuentes, J.L. Nava, O. Coreño, Y. Li, J.H. Hernández, Simultaneous removal of fluoride and arsenic from groundwater by electrocoagulation using a filter-press flow reactor with a three-cell stack, Sep. Purif. Technol., 208 (2019) 208–216.
[85] A. Guzmán, J.L. Nava, O. Coreño, I. Rodríguez, S. Gutiérrez, Arsenic and fluoride removal from groundwater by electrocoagulation using a continuous filter-press reactor, Chemosphere, 144 (2016) 2113–2120.
[86] A. Betancor-Abreu, V.F. Mena, S. González, S. Delgado, R.M. Souto, J.J. Santana, Design and optimization of an electrocoagulation reactor for fluoride remediation in underground water sources for human consumption, J. Water Process Eng., 31(2019) 100865, doi: 10.1016/j.jwpe.2019.100865.